

# DOE-EPSCoR Final Report

Period: September 1, 2008- August 31, 2016

## Development and Understanding of Multifunctional Nanostructured Magnetoelectric and Spintronic Materials

(DOE-EPSCoR Award #DE-FG 02-08ER46526)

**Date of the Report:** October 31, 2016

**Award period covered by the report:** September 1, 2008- August 31, 2016

### Investigators

R.S. Katiyar (PI)<sup>1</sup>, M. Gomez<sup>1</sup>, G. Morell<sup>1</sup>, L. Fonseca<sup>1</sup>, Y. Ishikawa<sup>1</sup>, R. Palai<sup>1</sup>, R. Thomas<sup>1</sup>, A. Kumar<sup>1</sup>, J. Velev<sup>1</sup>, V. Makrov<sup>1</sup>, O. Perales<sup>2</sup>, M.S. Tomar<sup>2</sup>, W. Otaño<sup>3</sup>.

<sup>1</sup>*University of Puerto Rico, Rio Piedras Campus*, <sup>2</sup>*University of Puerto Rico, Mayaguez Campus*; <sup>3</sup>*University of Puerto Rico, Cayey Campus*

### Research Focus:

*In this project, multifunctional nanostructured spintronic and magnetoelectric materials were investigated by experimental and computational efforts for applications in energy efficient electronic systems that integrate functionalities and thus have the potential to enable a new generation of faster responding devices and increased integration densities. The team systematically investigated transition metal (TM)-doped ZnO nanostructures, silicide nanorods, magnetoelectric oxides, and ferroelectric/ferromagnetic heterostructures.*

In what follows, we report the progress made by researchers during the above period in developing and understanding of 1) Spintronics nanostructures; 2) Resistive switching phenomenon in oxides for memory devices; 3) Magnetoelectric multiferroics; 4) Novel high-k gate oxides for logic devices; 5) Two dimensional (2D) materials; and 6) Theoretical studies in the above fields.

### A brief description of accomplishments

#### 1. Spintronics Nanostructures:

##### 1.1 Synthesis of ZnO thin films with controlled density and composition of structural defects

High quality ZnO thin films with controlled density and composition of structural defects were deposited on c-sapphire and oxidized silicon substrates by dc pulsed reactive sputtering using 40 W of power and 600 °C substrate temperature. The X-ray diffraction (XRD) and the photoluminescence (PL) characteristics of ZnO thin films grown at various oxygen to argon ratios was studied to study point defects in the films and their relation to the magnetic behavior. We also studied the effect of the oxidation state of Fe species and the influence of the annealing atmosphere on the structural and functional properties of nanocrystalline ZnO-based powders. The formation of pure and Fe-doped ZnO nanocrystalline powders were confirmed by XRD, UV-Vis and PL measurements. No isolated impurity phases were detected. TEM analyses confirmed the formation of nanosize particles in the 10-20 nm range. PL spectra of bare and Fe-doped ZnO powders evidenced the main emission band in the UV region. The quenching-by-concentration effect observed was attributed due to the formation of trapping states by the dopant species. Fe<sup>3+</sup>-doped ZnO exhibited weak but noticeable room-temperature ferromagnetism. These results open interesting possibilities for the use of Fe-doped ZnO in multifunctional systems and devices.

##### 1.2 Synthesis and magnetic characterization of silicide nanowires

Using chlorine precursors and (100) silicon substrates, nanowires of FeSi, CoSi, Fe<sub>x</sub>Mn<sub>1-x</sub>Si, and Co<sub>x</sub>Mn<sub>1-x</sub>Si were fabricated in a two zone CVD furnace with temperatures and pressures ranging from 800 - 1200 °C and 500 -

760 Torr. It resulted into nanowires with diameters of 500nm – 40nm that had shown magnetic response at different temperatures, measured using a Vibrating Sample Magnetometer (VSM). Magnetic domain measurements were also carried out on a single nanowire, using a Magnetic Force Microscope (MFM). Density functional theory was implemented to understand the origin of the magnetism on the nanowires. The calculations were performed using the Vienna Ab initio simulation package (VASP). Results show magnetization on the surface atoms of a FeSi (111) slab.

### 1.3 Thin films of ZnO for multifunctional applications

ZnO thin films were deposited on c-sapphire and oxidized silicon substrates by dc pulsed reactive sputtering using low power values and 600°C of substrate temperature in order to produce the lowest arrival rate possible and the highest substrate temperature ( $T_s > 1/3 T_m$ ) necessary to increase the adatom mobility. Manganese doping was achieved by rf co-sputtering with a second gun. The average thickness of the samples was 250 nm. XRD shows high (002) crystal orientation and a shift in the peak position toward smaller angles, possibly as a result of the substitutional incorporation of the larger Mn ions. EDS and XPS analysis were used to measure the amount of Mn in the films. A new set of samples was prepared where all contamination sources were reduced 10-fold or eliminated. These samples, and a new set with increased Zn deposition rate and oxygen content, and decreased substrate temperature, are scheduled to be characterized with RBS and magnetic measurements, during the summer, to correlate the density of defects in the sample with the appearance of the ferromagnetic signal.

A systematic study was carried out to determine the effect of composition and annealing atmosphere (air and  $N_2$ ) on the structural, optical and magnetic properties of pure, doped and co-doped ZnO [ $Zn_{(1-y)}(CoV)_yO$ ] nanocrystalline powders and films. The XRD pattern of films show enhancement of crystallinity with annealing under  $N_2$  atmosphere. Magnetic studies reveal a weak ferromagnetism in all V- and (Co+V)-doped ZnO/Si(100) films, annealed at 500 °C in air. However, the films annealed under  $N_2$  atmosphere at same temperature show a large enhancement of ferromagnetism and coercivity and the (Co+V)-doped films show further enhancement of ferromagnetism than V-doped films. This ferromagnetic behavior may be attributed to the super exchange interaction through oxygen ions or to the exchange interaction between spins of the band carriers and localized spins of Co and V; Cobalt ions contribute to the saturation magnetization with  $6\mu_B$  and Vanadium ions with  $4/3\mu_B$  per ion. The PL spectra of films show weak defect band in the films and this defect-induced ferromagnetism is explained in terms of the bound magnetic polarons model (BMP) applied to oxide DMS's

### 1.4 Magnetic structure and interactions in (Sb, Co) co-doped ZnO thin films

The magnetic behaviour of (Co, Sb) co-doped ZnO thin films grown by pulsed laser deposition was investigated. The irreversibility (ZFC–FC bifurcation) in low field ( $H = 100$  Oe) magnetization and small hysteresis below 300 K are similar in samples with or without Sb co-doping. Both the phenomena originated from the presence of blocked supermoments in the samples. Incorporation of Sb only increases the saturation magnetization and coercivity. The quantitative increase in moment due to Sb co-doping suggests a transfer of electrons from Co ions to Sb-related acceptor complexes. This is supported by a decrease in the number of electronic transitions from Co d electrons to the conduction band seen in optical transmission spectroscopy when Sb is added. The high field susceptibility data show the existence of supermoments with antiferromagnetic interaction between them. We found that the value of the effective antiferromagnetic molecular field constant decreases with increasing Co concentration, revealing that the supermoments are bound magnetic polarons around intrinsic donors, rather than coming from Co precipitates. True ferromagnetism (overlapping polarons) can emerge either with larger intrinsic donors, or with acceptors with shallower levels, than those created by Sb co-doping. Our results suggest that Sb-related acceptor states may be unstable towards accepting electrons from deep d levels of Co ions.

### 1.5 Dilute magnetic semiconductor (DMS): RE-doped InGaN Nanostructures

Thin films of Er and Yb doped GaN were successfully grown by plasma assisted MBE under different doping concentrations (4-10%) and thickness (50, 100, and 150 nm) for spintronic and optoelectronic applications. The GaN:Yb thin films are found to be ferromagnetic at room temperature, but the GaN:Er thin films are ferromagnetic below 175 K. Furthermore, while the thicker films with higher doping concentration of Er and Yb ions showed good ferromagnetic properties, they showed weak photoluminescence properties. A prototype magnetic semiconductor tunnel junction (MTJ), GaYbN/AlN/GaYbN (150nm/2nm/150nm), was fabricated by MBE. The tunnelling magnetoresistance (TMR) was found to be 7.6% at RT that increased with lowering temperature. High In-content

InGaN with Yb and Er doping were also successfully grown using MBE. Yb:InGaN thin films show excellent PL spectra without any defect bands.

It was found that adding RE elements to the ammonia solution during GaN ammonothermal growth process resulted in a substantial improvement in the optical properties of grown GaN crystals due to the gettering of oxygen and other impurities. Since the 4f electrons are very localized, the RE elements retain the same chemical activity irrespective of the host, and have magnetic moment than transition metal, and might attract defects and intrinsic impurities creating complexes in epitaxial films, similar in nature to the gettering effect. We explored Yb-doped high indium content InGaN semiconductor. The diffraction (RHEED) patterns recorded during and after the growth revealed crystalline nature of the nanorods. The nanorods were examined using high resolution electron microscopy (HRTEM) and atomic force microscopy. The photoluminescence studies of the nanorods showed the visible emissions. The In composition was calculated from the photoluminescence measurements using Vegard's law and found to be 38.4% for InGaN and 39.5% for Yb ( $\pm 5\%$ )-doped InGaN with a bowing parameter  $b = 1.01\text{eV}$ . The Yb-doped InGaN showed significant enhancement in photoluminescence properties compared to the undoped InGaN. The Yb-doped InGaN nanorods demonstrated the shifting of the photoluminescence band at room temperature. The magnetic properties studied using the superconducting quantum interference device (SQUID) shows room temperature ferromagnetic behaviour.

### 1.6 Quantum Filter of Spin Polarized State Device

In collaboration with Dr. Igor V. Khmelinskii (Universidade do Algarve, FCT, DQF, and CIQA, Faro P8005-139, Portugal), in 2013 we continued studies of Quantum Filter of Spin Polarized State Device (AFSPSD) based on multilayer sandwich structured interfaces. Presently we report spin-polarized state transport in Metal – Dielectric – Iron (MDFe), Metal – Dielectric – Semiconductor (1) (MDS1) and Metal – Dielectric – Semiconductor (2) (MDS2) three-nanolayer sandwich devices. The exchange-resonance spectra in such devices are quite specific, differing also from spectra observed in other three-nano-layer devices. The published theoretical model was extended and used to interpret the available experimental results. A detailed ab initio analysis of the magnetic-field dependence of the output magnetic moment averaged over the surface of the device was as well performed. The model predicts the resonance structure of the output signal. Structure of resonance is dependent of different reasons. Developed by us theory allowed to explain of the observed differences between simulated and observed spectra and fit experimental spectra with acceptable accuracy. We developed phenomenological and ab initio theoretical approaches to explain the observed phenomenon. The phenomenological approach gave significantly better fitting of experimental spectra than ab initio analysis.

A novel method for the measurement of g-factor and spin-lattice relaxation time of spin-polarized states in nano-layers of different chemical nature was developed. This method is based on usage of spin-polarized state quantum filter, which was created and tested earlier [V. I. Makarov et al., J Appl. Phys. 110, 063717 (2011) and V. I. Makarov et al., J Appl. Phys. 112, 084310 (2012)]. The spin state parameters were measured in nanolayers of different materials (Fe, Au, and Si) in function of such experimental parameters as the layer thickness and temperature. The phenomenological model developed earlier for steady-state conditions was presently extended to include time dependence and successfully used in the data analysis. Qualitative models were proposed that explain the observed dependences, forming the basis for future theoretical developments.

### 1.7 Transition metal doped ZnO thin films

ZnO based dilute magnetic semiconductors (DMS) for the novel magneto electronic devices were screened with various doping levels. The ZnCuO films showed nearly single crystalline phase ( $\leq 3\%$  Cu doping) with ferromagnetic behavior ( $M_s \sim 0.76 \mu_B/\text{Cu}$ ) that reduced on further increase in Cu doping. Moreover, the 1%Cu doped ZnO thin film is epitaxial and free from any interfacial reaction with the alumina substrate. The high- $T_c$  ferromagnetic property in Co-doped ZnO (ZCO), mediated by donor impurity band was tested by the controlled introduction of shallow donors (Al) in the  $\text{Zn}_{0.9-x}\text{Co}_{0.1}\text{O:Al}_x$  ( $x = 0.005$  and  $0.01$ ) thin films. The saturation magnetization for the 10% Co-doped ZnO (4emu/cc) at 300 K reduced ( $\sim 0.8 \text{ emu/cc}$ ) due to Al doping and the resistivity dropped abruptly, from  $\sim 10^3 \Omega\text{-cm}$  for the ZCO film to 0.033 and  $0.02 \Omega\text{cm}$  for the 0.5% and 1.0% Al doped ZCO samples respectively. The optical band gap in the Mn-doped (1-10%) ZnO was found to increase (3.27 eV to 3.41 eV) due to Mn doping. Recently, we synthesized Antimony (Sb 3% and 5%) doped *p*-type ZnO films that exhibited **high hole concentration** of  $6.25 \times 10^{18} \text{ cm}^{-3}$ , mobility of  $57.44 \text{ cm}^2/\text{Vs}$ , and low resistivity ( $\Omega \text{ cm } 0.017$ ) in the 5% Sb-doped ZnO thin film.

**1.8 Nano-structured fibers and ribbons:** The electrospinning technique has been used to fabricate ZnO and ZnO [Fe, Mn] fibers and ribbons. After a careful study of the synthesis process it was shown that specific variations in the composition of the precursor solution allows the production of different morphologies ranging from droplets to fibers and ribbons. In addition, it was possible to add specific amounts of Fe or Mn to the solution to produce specific doping levels in the ribbons. In a separate set of experiments, it was shown that it is possible to change the polycrystalline texture of ZnO nanowires deposited by dc sputtering by changing the plasma deposition conditions. The variation in fiber morphology is obtained by control of the polymer/salt solution used in the electrospinning process. Different polymer concentrations are correlated to variations in the magnetization properties of the fibers. ZnFe<sub>2</sub>O<sub>4</sub> and CrFe<sub>2</sub>O<sub>4</sub> micro-to-nanometer size fibers, in particular, have been successfully fabricated.

a) ZnO:Fe A complete study has been completed on the solution-parameter conditions required to produce different morphologies, from droplets to fibers, in the electrospinning technique. The ratio of (poly) ethylene oxide to Fe: Zn was used to control the formation of ribbon and fiber morphologies.

b) ZnFe<sub>2</sub>O<sub>4</sub> spinel was prepared by the electrospinning technique using sol-gel precursors with different polymers. The electrospun fibers were heated in air at different temperatures to eliminate the solvent and polymer while growing the desired crystalline material. During the heat treatment, the ferrite crystal is nucleated and thermally driven toward the growth of the spinel cubic crystals. In this process oxygen is incorporated and the formation of the fiber appears to be completed at 600° C. The XRD spectra confirmed the zinc ferrite formation in the cubic spinel structure with an increase in the intensity signal with temperature. The SEM images of ZnFe<sub>2</sub>O<sub>4</sub> show the formation of fibers and ribbons in a diameter range of 100 to 500 nm.

Magnetic hysteresis loops of ZnFe<sub>2</sub>O<sub>4</sub> samples heat-treated at 300, 400, 500, 600, 700, and 800 °C were measured at room temperature using the vibrating sample magnetometer (VSM) and the typical hysteresis loops as a function of heat-treatment were observed. The samples show the characteristic hysteresis response of magnetic materials where the saturation moment increases with temperature. Magnetization, remnance and coercivity increased with increasing the heat-treatment temperature. The ribbons had a small increase in magnetic response as compared with fibers, a result that requires further study. The sample heat-treated to 800 °C showed a significantly higher saturation magnetization as compared with the other ones. It is speculated that the increase in magnetic response is a consequence of the segregation of the Fe<sub>2</sub>O<sub>3</sub> phase with nanocrystallite size.

## 2. Resistive switching Phenomenon in Oxides for Memory Devices

### 2.1 Nonpolar resistive switching in amorphous ternary rare-earth LaHoO<sub>3</sub> thin films

We studied the resistive memory switching in pulsed laser deposited amorphous LaHoO<sub>3</sub> (a-LHO) thin films for non-volatile resistive random access memory (RRAM) applications. Nonpolar resistive switching (RS) was achieved in Pt/a-LHO/Pt memory cells with all four possible RS modes (i.e., positive unipolar, positive bipolar, negative unipolar, and negative bipolar) (Fig. 2) having high R<sub>ON</sub>/R<sub>OFF</sub> ratios (in the range of ~10<sup>4</sup>-10<sup>5</sup>) and non-overlapping switching voltages (set voltage, V<sub>ON</sub> ~ ± 3.6-4.2 V and reset voltage, V<sub>OFF</sub> ~ ± 1.3-1.6 V) with a small variation of about ± 5-8%. Temperature dependent current-voltage (I-V) characteristics indicated the metallic conduction in low resistance states (LRS). We propose that the formation (set) and rupture (reset) of mixed conducting filaments formed out of oxygen vacancies and metallic Ho atoms could be responsible for the change in the resistance states of the memory cell. Detailed analysis of I-V characteristics further corroborated the formation of conductive nano-filaments based on metal-like (Ohmic) conduction in LRS. Simmons-Schottky emission was found to be the dominant charge transport mechanism in the high resistance state.

### 2.2 Unipolar resistive switching behavior of amorphous YCrO<sub>3</sub> films

Amorphous YCrO<sub>3</sub> (YCO) films were prepared on Pt/TiO<sub>2</sub>/SiO<sub>2</sub>/Si substrate by pulsed laser deposition in order to investigate resistive switching (RS) phenomenon. The Pt/YCO/Pt device showed stable unipolar RS with resistance ratio of ~10<sup>5</sup> between low and high resistance states, excellent endurance and retention characteristics, as well as, non-overlapping switching voltages with narrow dispersions. Based on the x-ray photoelectron spectroscopy and temperature dependent switching characteristics, observed RS was mainly ascribed to the oxygen vacancies. Moreover, current-voltage characteristics of the device in

low and high resistance states were described by Ohmic and trap controlled space-charge limited conduction mechanisms, respectively.

### **2.3 Enhanced resistive switching in graphene oxide films embedded with gold nanoparticles**

Forming-free resistive random access memory (ReRAM) devices having low switching voltages are a prerequisite for their commercial applications. In this study, the forming-free resistive switching characteristics of graphene oxide (GO) films embedded with gold nanoparticles, having an enhanced on/off ratio at very low switching voltages, were investigated for non-volatile memories. The GOAu films were deposited by the electrophoresis method and as-grown films were found to be in the low resistance state; therefore, no forming voltage was required to activate the devices for switching. The devices having an enlarged on/off ratio window of  $\sim 10^6$  between two resistance states at low voltages ( $< 1$  V) for repetitive dc voltage sweeps showed excellent properties of endurance and retention. In these films gold nanoparticles were uniformly dispersed over a large area that provided charge traps, which resulted in improved switching characteristics. Capacitance was also found to increase by a factor of  $\sim 10$ , when comparing high and low resistance states in GOAu and pristine GO devices. Charge trapping and de-trapping by Au Nps was the mechanism responsible for the improved switching characteristics in the films.

### **2.4 Resistive switching properties of doped $\text{BiFeO}_3$ thin films:**

The variation of Cr-dopant concentration in BFO was found to alter the structural, optical, magnetic and resistive switching properties to different extents in pulsed laser deposited  $\text{BiFeO}_3$  (BFCO) films. BFCO thin films showed higher optical band gap, improved magnetization behavior owing to super exchange interaction between aliovalent Cr and Fe-ions, and lower leakage current with increased Cr-doping concentration. BFCO films with higher Cr-concentrations were not found to show resistive switching ascribed to the high valance  $\text{Cr}^{4+}$ -ion induced annihilation of oxygen vacancies, which exhibit the crucial role of oxygen vacancies towards resistive switching phenomenon in BFO thin films.

## **3. Magnetoelectric Multiferroics**

### **3.1 Photovoltaic studies in multiferroic thin films**

We studied photovoltaic effect and multiferroic properties of a  $0.9(\text{BiFeO}_3)-0.1(\text{YCrO}_3)$  composite thin films deposited on a  $\text{Pt}/\text{TiO}_2/\text{SiO}_2/\text{Si}$  substrate by sequential ablation of  $\text{BiFeO}_3$  and  $\text{YCrO}_3$  ceramic targets using pulsed laser deposition. The desired composition of the composite was achieved by controlling the ablation time of respective targets. The enhanced saturation magnetization compared to pristine polycrystalline films was attributed to the super-exchange interactions between Fe and Cr-ions. The photovoltaic properties of the composite thin film were studied under white light illumination in both top-bottom and lateral electrode configurations. Short circuit current densities ( $\text{JSC}$ ) =  $1.48 \mu\text{Acm}^{-2}$  and  $0.44 \mu\text{Acm}^{-2}$ , and open circuit voltages ( $\text{VOC}$ ) =  $0.51$  V and  $0.32$ V were observed in top-bottom and lateral electrode configurations, respectively.

We have studied photovoltaic properties of codoped ferroelectric  $[\text{Bi}_{0.9}\text{La}_{0.1}][\text{Fe}_{0.97}\text{Ti}_{0.02}\text{Zr}_{0.01}]\text{O}_3$  (BLFTZO) thin films. Polycrystalline BLFTZO films were fabricated on  $\text{Pt}/\text{TiO}_2/\text{SiO}_2/\text{Si}$  substrates by pulsed laser deposition technique. Al-doped  $\text{ZnO}$  transparent top electrodes complete the  $\text{ZnO:Al}/\text{BLFTZO}/\text{Pt}$  metal-ferroelectric-metal capacitor structures. BLFTZO showed switchable photoresponse in both polarities. The open circuit voltage ( $\text{VOC}$ ) and short circuit current ( $\text{JSC}$ ) were found to be  $\sim 0.022$ V and  $\sim 650$   $1\text{A}/\text{cm}^2$ , respectively after positive poling, whereas significant difference in  $\text{VOC} \sim 0.018$ V and  $\text{JSC} \sim 700$   $1\text{A}/\text{cm}^2$  was observed after negative poling. The observed switchable photocurrent and photovoltage responses are explained on the basis of polarization flipping in BLFTZO due to the applied poling field.

We have also studied switchable photovoltaic and photo-diode characteristics of  $\text{Pt}/(\text{Bi}_{0.9}\text{Sm}_{0.1})(\text{Fe}_{0.97}\text{Hf}_{0.03})\text{O}_3/\text{LaNiO}_3$  ( $\text{Pt}/\text{BSFHO}/\text{LNO}$ ) heterostructures integrated on Si (100). The directions of photocurrent ( $\text{JSC}$ ) and rectification are found to be reversibly switchable after applying external poling voltages. In pristine state, metal-ferroelectric-metal capacitor  $\text{Pt}/\text{BSFHO}/\text{LNO}$  shows  $\text{JSC} \sim 32 \mu\text{A}/\text{cm}^2$  and  $\text{VOC} \sim 0.04$  V, which increase to maximum value of  $\text{JSC} \sim 303$  ( $-206$ )  $\mu\text{A}/\text{cm}^2$  and  $\text{VOC} \sim -0.32$  ( $0.26$ ) V after upward (downward) poling at  $\pm 8$  V. We believe that the Schottky barrier modulation by polarization flipping at  $\text{Pt}/\text{BSFHO}$  interface could be a main

driving force behind switchable photovoltaic and rectifying diode characteristics of Pt/BSFHO/LNO heterostructures.

### 3.2 Tunneling electroresistance in multiferroic heterostructures

We have observed room temperature polar switching and tunneling in  $\text{PbZr}_{0.52}\text{Ti}_{0.48}\text{O}_3$  (PZT) ultra-thin films of thickness 3–7 nm, sandwiched between platinum metal and ferromagnetic  $\text{La}_{0.67}\text{Sr}_{0.33}\text{MnO}_3$  (LSMO) layers, which also shows magnetic field dependent tunnel current switching in  $\text{Pt/PbZr}_{0.52}\text{Ti}_{0.48}\text{O}_3/\text{La}_{0.67}\text{Sr}_{0.33}\text{MnO}_3$  heterostructures. The epitaxial nature, surface quality and ferroelectric switching of heterostructured films were examined with the help of x-ray diffraction patterns, atomic force microscopy, and piezo force microscopy, respectively. The capacitance versus voltage graphs show butterfly loops above the coercive field ( $>\pm 3$  V) of PZT for small probe area ( $\sim 16 \mu\text{m}^2$ ). The effect of ferroelectric switching was observed in current density versus voltage curves with a large variation in high-resistance/low-resistance (HRS/LRS) ratio (2:1 to 100:1), however, these effects were more prominent in the presence of in-plane external magnetic field. The conductance is fitted with Brinkman's model, and the parabolic conductance upon bias voltage implies electron tunneling governs the transport.

Self-poled ultra-thin ferroelectric  $\text{PbZr}_{0.52}\text{Ti}_{0.48}\text{O}_3$  (PZT) (5 and 7 nm) films have been grown by pulsed laser deposition technique on ferromagnetic  $\text{La}_{0.67}\text{Sr}_{0.33}\text{MnO}_3$  (LSMO) (30 nm) to check the effect of polar capping on magnetization for ferroelectric tunnel junction devices. PZT/LSMO heterostructures with thick polar PZT (7 nm) capping show nearly 100% enhancement in magnetization compared with thin polar PZT (5 nm) films, probably due to excess hole transfer from the ferroelectric to the ferromagnetic layers. Core-level x-ray photoelectron spectroscopy studies revealed the presence of larger Mn 3s exchange splitting and higher  $\text{Mn}^{3+}/\text{Mn}^{4+}$  ion ratio in the LSMO with 7 nm polar capping.

### 3.3 $\text{Sr}_2\text{FeMoO}_6$ Based Tri-layer Structures for Magnetoresistive Applications

Tunnel magnetoresistance in  $\text{Sr}_2\text{FeMoO}_6$  based tri-layered structure was studied at room temperature. The  $\text{Sr}_2\text{FeMoO}_6/\text{SrTiO}_3/\text{Sr}_2\text{FeMoO}_6$  tri-layered structure was grown by pulse laser deposition on STO buffered Si(100) substrate. The X-ray diffraction and Micro Raman studies confirm the polycrystalline phase formation of SFMO thin films without any impurity phases. The single layer SFMO thin film shows the good ferromagnetic behavior with saturation magnetization of  $\sim 1.48 \mu\text{B}/\text{f.u.}$  at room temperature. The high value of tunneling magnetoresistance of  $\sim 7\%$  of tri-layer structure at room temperature was attributed to spin dependent tunneling through uniform STO barrier layer. The room temperature tunneling magnetoresistance in SFMO tri-layer structure open the future prospect for their possible integration to room temperature spintronic devices.

### 3.4 Magnetoelectric and magnetodielectric studies in multiferroics

Our research has been focused on investigating magnetoelectric and magnetodielectric couplings in multiferroic materials listed below:

*Rare-earth (Sm, Dy) and transition metal (Co) modified polycrystalline  $\text{BiFeO}_3$*

*Solid solutions of PZT with  $\text{Pb}(\text{Fe}_{1/2}\text{Nb}_{1/2})\text{O}_3$  (PFN),  $\text{Pb}(\text{Fe}_{1/2}\text{Ta}_{1/2})\text{O}_3$  (PFT), and  $\text{Pb}(\text{Fe}_{2/3}\text{W}_{1/3})\text{O}_3$  (PFW)*

*$\text{Pb}(\text{Zr}_{0.20}\text{Ti}_{0.80})_{0.70}\text{Pd}_{0.30}\text{O}_{3-\delta}$  (PZTPd);  $(\text{Bi}_{0.95}\text{Nd}_{0.05})(\text{Fe}_{0.97}\text{Mn}_{0.03})\text{O}_3$  (BNFM)*

*$\text{Pb}(\text{Fe}_{0.5}\text{Nb}_{0.5})\text{O}_3/\text{Ni}_{0.65}\text{Zn}_{0.35}\text{Fe}_2\text{O}_4/\text{Pb}(\text{Fe}_{0.5}\text{Nb}_{0.5})\text{O}_3$  (PFN/NZFO/PFN)*

Rare-earth (Sm, Dy) and transition metal (Co) modified polycrystalline  $\text{BiFeO}_3$  (BFO) thin films were deposited on  $\text{Pt/TiO}_2/\text{SiO}_2/\text{Si}$  substrates successfully utilizing pulse laser deposition (PLD) technique. Piezoelectric, leakage current and temperature dependent dielectric and magnetic behavior were investigated. Typical butterfly-shaped loops were observed in polycrystalline films with effective piezoelectric constant ( $d_{33}$ )  $\sim 94 \text{ pm/V}$  at 0.6 MV/cm. High dielectric constant  $\sim 900$  and low dielectric loss  $\sim 0.25$  were observed at room temperature. M–H loop had shown relatively high saturation magnetization  $\sim 35 \text{ emu/cm}^3$  at a maximum field of  $H\sim 20 \text{ kOe}$ . Enhanced magnetoelectric coupling response was observed under applied magnetic field compared to polycrystalline pure BFO. However, the single domain BFO single crystal showed very strong magnetoelectric coupling and  $\sim 40\%$  change in magnetopolarization  $\{\text{MP} = [\text{Ps}(\text{H})-\text{Ps}(0)]/\text{Ps}(0)\}$ .

A novel single phase-pure PZTP30 magnetoelectric having tetragonal crystal structure with  $\text{P}4\text{mm}$  symmetry was considered for possible room temperature multi-states tunable logic and nonvolatile memory elements under external E and M-fields. It possesses high magneto-electric coefficients  $\sim 0.36 \text{ mV/cm.Oe}$  at  $H_m= 3 \text{ kOe}$  in a single-phase system suggesting a strong coupling between piezo- and magneto-striction at nanoscale. It displays room-

temperature weak ferromagnetism, strong ferroelectricity, and strong ME coupling. We believe the origin of magnetism is due to mixed valance states of the  $\text{Pd}^{2+}/\text{Pd}^{4+}$  in PZT matrix as confirmed by XPS and XRF studies. A sharp ferroelectric-paraelectric phase transition is observed near 569 K, well supported by dielectric, Raman, and thermal studies. The giant room-temperature magneto-electric coupling makes it a future alternative of  $\text{BiFeO}_3$  with a strong possibility for real device applications.

We have also studied magnetic properties and conduction mechanisms of Nd and Mn co-doped  $\text{BiFeO}_3$  ( $\text{Bi}_{0.95}\text{Nd}_{0.05}(\text{Fe}_{0.97}\text{Mn}_{0.03})\text{O}_3$ ) (BNFM) polycrystalline electroceramics. Magnetic studies have been carried out in two different temperature regions i.e. 15-300 K and 300-800 K. The substitution of Nd and Mn in the  $\text{BiFeO}_3$  (BFO) lattice slightly reduces the Néel temperature (TN) by increasing ferromagnetic domain fractions, causes enhancement in magnetization. A small amount of magnetic frustration is also found in the low temperature regions, below 300 K at fields of 100 and 200 Oe, and below 200 K at higher field cooled (FC) and zero field cooled (ZFC) samples; this may be due weak long range ordering and small magnetic moments. High temperature magnetic results imply the existence of a weak ferromagnetic phase with a ferromagnetic to paramagnetic transition around 630 K (+/- 5 K) and significant suppression of the spin frustration and canting properties of BFO. The Nd and Mn substitutions also substantially improved the electrical insulating properties of BFO. The leakage current conduction mechanisms were analyzed in the insulating ceramic capacitors in the light of conventional models. The leakage current analysis yields the conduction mechanism of BNFM is consistent with a tunneling behavior and the electronic current may be predicted by Simmons' model over a wide temperature range from 80 to 350 K. The observed results not only give better insight into the conduction mechanisms and spin dynamics of BFO through site engineering, but also can facilitate for the potential multifunctional and spintronics device applications.

**Multiferroic trilayer heterostructures:** Multiferroic Magnetoelectrics (MF-ME) have attracted considerable attention since its rediscoveries as possible candidates for a wide variety of future electronic and memory devices, although robust magnetoelectric (ME) coupling between electric and magnetic orders at room temperature still remains difficult to achieve. In continuation to our investigations for achieving robust ME coupling at room temperature we have studied FE/FM/FE trilayer heterostructure. Here we report the tip induced polarization switching and ME properties of  $\text{Pb}(\text{Fe}_{0.5}\text{Nb}_{0.5})\text{O}_3/\text{Ni}_{0.65}\text{Zn}_{0.35}\text{Fe}_2\text{O}_4/\text{Pb}(\text{Fe}_{0.5}\text{Nb}_{0.5})\text{O}_3$  (PFN/NZFO/PFN) trilayer nanoscale heterostructure having dimension 70/20/70 nm, respectively at room temperature. The presence of only (00l) reflection of PFN and NZFO in the XRD patterns and electron diffraction patterns in TEM confirm the epitaxial growth of multilayer heterostructure. The existence of ferroelectricity and tip induced polarization switching at nanoscale has been confirmed by band excitation piezo force microscopy (BE-PFM) studies. The distribution of the ferroelectric loop area in a wide area has been studied, suggesting that spatial variability of ferroelectric switching behaviour is low, and film growth is of high quality. The ferroelectric and magnetic phase transitions of these heterostructures have been found at ~575 K and ~650 K, respectively which are well above room temperature. These nanostructures exhibit low loss tangent, large saturation polarization ( $\text{Ps} \sim 38\mu\text{C}/\text{cm}^2$ ) and magnetization ( $\text{Ms} \sim 48\text{ emu}/\text{cm}^3$ ) with strong ME coupling at room temperature elucidate the possible potential candidates for multifunctional and spintronics nanoscale device applications.

### **3.5 Domain studies by Piezoresponse Force Microscopy (PFM) and SEMPA:**

We used Band excitation Piezoresponse Force Microscopy (PFM) and Switching Spectroscopy PFM (SS-PFM) for understanding surface physics and domain dynamics (switching, domain type, domain growth, retention, and fatigue) properties of - aforementioned structures. The domain dynamics study results were compared with the magnetoelectric measurements for better understanding of the ME coupling in multiferroics.

The existence of ferroelectric polarization Switching in  $\text{Pb}(\text{Fe}_{0.5}\text{Nb}_{0.5})\text{O}_3 - x \text{ Ni}_{0.65}\text{Zn}_{0.35}\text{Fe}_2\text{O}_4$  ( $x=0-0.4$ ) composite thin films was confirmed by the band excitation Piezo Force Microscopy (PFM). PFM images showed clear and reversible out-of-plane phase contrast above  $\pm 5$  V, which indicates the ferroelectric character of those thin films. In order to further confirm the existence of ferroelectricity, piezoresponse as a function of tip bias measurements in read (out of field), write (in field) and (infield- out of field) measurements has been done. All films showed noticeable piezoresponse.

The local polarization reversal of PFN by an electric field produced by a conductive SPM tip as a function of the relative humidity and temperature in an SPM chamber has been studied. The decrease of piezoresponse is observed with increase of relative humidity and temperature. The observed phenomena are attributed to the existence of a water meniscus in the vicinity of the tip-surface contact. These results are important for a deeper understanding

of complex investigations of ferroelectric materials and their applications and suggest the necessity for fundamental studies of electrocapillary phenomena at the tip-surface junction and their interplay with bias-induced materials responses. The ferroelectric phase transition is also probed by the temperature dependence of piezoresponse studies. In addition to the temperature dependence of piezoresponse studies the phase transition is also confirmed by temperature dependent dielectric spectra. The temperature dependent and humidity dependent piezoresponse and dielectric spectra of all composite thin films unearth many important physics.

We have also investigated the growth of multifunctional perovskite oxide  $\text{BiFeO}_3$  (BFO) epitaxial thin films on orthorhombic (100)  $\text{NdGaO}_3$  (NGO) single-crystal substrates. The ferroelectric and ferroelastic properties of BFO thin films structures were studied using atomic force microscopy techniques. We observed long range ordering of ferroelectric  $109^\circ$  stripe nanodomains separated by periodic vertical domain walls in as grown BFO films. We found that B-site doping of Nb-ions changes the nature of the stripe domain walls from  $109^\circ$  to  $71^\circ$  in Nb-doped (110) BFO film epitaxially grown on NGO. Such strain field driven long-range periodic stripe ferroelectric/ferroelastic domains are useful for opto-electronic devices and ferroelastic templates for strain coupled artificial magnetoelectric heterostructures.

### 3.6 Multiferroic Heterostructures

Artificially synthesized ferroelectric/ferromagnetic heterostructures and superlattices of ferroelectric,  $\text{Ba}_{1-x}\text{Sr}_x\text{TiO}_3$  (BSTO),  $T_c \sim 310\text{K}$  and CMR manganites (ferromagnetic),  $\text{La}_{2/3}\text{Sr}_{1/3}\text{MnO}_3$  (LSMO),  $T_c \sim 350\text{K}$  were using pulsed laser deposition. Our fabricated heterostructures using 20nm thick LSMO/BSTO/LSMO show multiferroic properties. The heterostructures also have systematically been investigated using several analytical techniques such as micro-Raman spectroscopy, X-ray photoelectron spectroscopy (XPS), atomic force microscopy, dielectric spectroscopy, and magneto-electric measurements for better understanding of structure-property relationship. Single-domain single crystals and thin films of multiferroic  $\text{BiFeO}_3$  on  $\text{SrTiO}_3$  substrates have systematically been studied using micro-Raman spectroscopy for better understanding of magnon-phonon coupling and dynamics of phase transition and phase diagram. A weak magnon-phonon coupling has been observed in BFO thin films at magnetic phase transition temperature. Thin films show the presence of a non-cubic  $\beta$ - and  $\gamma$ -phases at high temperature and no decomposition was observed up to  $1000\text{oC}$  thermal cycles. Thin films and polycrystalline samples of PFT have been investigated using several analytical techniques (SQUID, MFM, THz, magneto-electric measurements). Polycrystalline samples of PFT show room temperature multiferroic properties, strong magnetodielectric coupling, and nanoscale ordering.

A composite bilayers and superlattice (nano-capacitor) was fabricated based on ferroelectric  $\text{PbZr}_{0.52}\text{Ti}_{0.48}\text{O}_3$  (PZT) and half-metallic oxide  $\text{La}_{0.67}\text{Sr}_{0.33}\text{MnO}_3$  (LSMO) with different staking periodicity. High remnant polarization ( $12\text{-}54\mu\text{C}/\text{cm}^2$ ), dielectric constant (400-1700), and well saturated magnetization were observed depending upon the deposition temperature and staking periodicity of the ferromagnetic layer and applied frequencies. Zero field cooling (ZFC) measurements showed existence of cusp in magnetization at low temperatures indicating spin-glass like behavior contrary to PZT/LSMO bilayer structure. Giant frequency-dependent change in dielectric constant and loss were observed above the ferromagnetic-paramagnetic temperature.

The frequency dependent dielectric anomalies are attributed to the change in metallic and magnetic nature of LSMO and also the interfacial effect across the bilayer. Magnetic control of ferroelectric interface was also observed in bilayers. As field  $H$  is increased, the hysteresis loop first broadens (becomes lossy) and then disappears at ca.  $H=0.34\text{T}$  and ambient temperatures, the process was reversible. The results are interpreted as due to not to magnetocapacitance but to the sharp negative magneto-resistance in LSMO at low magnetic fields, which causes a dramatic increase in leakage current through the PZT.

The dielectric, magnetic, electrical, and dynamic magnetoelectric properties of ferroelectric (FE)  $\text{Pb}(\text{Zr},\text{Ti})\text{O}_3$  (PZT) and ferromagnetic (FM)  $\text{CoFe}_2\text{O}_4$  (CFO) thin films multilayers (MLs) with 3, 5, 9 layers were fabricated by pulsed laser deposition technique and characterize by impedance, dielectric and modulus spectroscopy. We observed two distinct electrical responses in all the investigated ML films at low temperature ( $<400\text{ K}$ ) and at the elevated temperature ( $>400\text{ K}$ ). We attributed these contributions to the grain effects <sup>(g)</sup> at low temperature and grain boundary <sup>(gb)</sup> effects at high temperature. We explained this electrical behavior by Maxwell-Wagner type contributions arising from the interfacial charge at the interface of the MLs structure. Master modulus spectra indicate that the magnitude of grain boundaries compare to grains become more prominent with increase in number of layer.

The frequency dependent conductivity results well fitted with the double power law,  $\sigma(\omega) = \sigma(0) + A_1\omega^{n_1} + A_2\omega^{n_2}$ , We observed a slow decrease in the polarization from 300 K to 200 K, complete collapse of polarization at  $\sim 100$  K, and complete recovery of polarization during heating, which was repeatable over hundreds of different experiments. Remanent magnetization of the layered nanostructure was three times higher at 100 K than at room temperature. A slow enhancement in remanent (internal) magnetization on lowering the temperature switched the polarization slowly until it collapsed. The temperature dependent dielectric, polarization and magnetization were different from the parent layer, indicating some kind of dynamic magneto-electric coupling in the layered nanostructures.

Dielectric films have attracted much attention for active and passive devices in silicon-based integrated circuits. Traditionally, dynamic random access memory (DRAM) capacitor and transistor gate uses highly scalable silicon based dielectrics such as  $\text{SiO}_2$ ,  $\text{SiO}_2/\text{Si}_3\text{N}_4$  and  $\text{Si}_3\text{N}_4$  in the planar geometries and lately in 3D structures.  $\text{DyScO}_3$  films were grown on platinized silicon and Si substrates by pulsed liquid injection MOCVD. Dielectric constant was around 22 and the capacitance was stable with the voltage, frequency and the temperature variation. These results suggest that  $\text{DyScO}_3$  films can be considered as high- $k$  material for and DRAM applications and buffer layer for MFIS devices. A significant amount of power is required for dynamic random access memories (DRAM) to refresh the capacitors compared to the non-volatile RAM (NVRAM). In fact, flash RAM currently dominates the market of non-volatile memories, but this memory is not as fast as DRAM and has a finite number of erase-write cycles. The polarization bistability of ferroelectric material offers the possibility to develop high-density, low power, faster write speed, maximum write-erase cycles and radiation resistance NVRAM; alternate to both DRAM and Flash. Hence, a gate-oxide with reasonable band offset ( $> 1\text{eV}$ ) may be the ideal choice as a buffer layer due to the fact that, the interface between Si and the ferroelectric is the main concern in reliable device applications. Considering these requirements of buffer layers, high- $k$  DSO gate-oxide seems to be promising for MFIS structures for non-volatile memory applications. We obtained DSO/p-Si(100) MIS structures with negligible CV hysteresis ( $< 5\text{ mV}$ ) and low leakage current density ( $6 \times 10^{-8}\text{ A/cm}^2$  at  $-2\text{ V}$ ). Multiferroic BFO thin film and high- $k$  DSO insulating buffer were fabricated on Si and the MFIS diodes were tested for the memory applications. The ferroelectric polarization of BFO gives rise to a memory window of  $1.7\text{ V}$ . The magnitude of the memory window demonstrates that BFO has potential in FET FeRAM applications. As a lead free ferroelectric,  $\text{Bi}_{3.25}\text{Nd}_{0.75}\text{Ti}_3\text{O}_{12}$  with  $\text{Pr} \sim 20.0\text{ }\mu\text{C/cm}^2$ ,  $E_c \sim 62\text{kV/cm}$ ,  $\epsilon_r \sim 400$  and  $\tan\delta \sim 0.04$  were successfully synthesized. MFIS diodes were fabricated by depositing  $\text{Bi}_{3.25}\text{Nd}_{0.75}\text{Ti}_3\text{O}_{12}$  ferroelectric film on p-type silicon substrate with an amorphous high- $k$   $\text{DyScO}_3$  film. The clockwise CV hysteresis and a memory window of about  $0.7\text{V}$  were obtained.

Layered nanostructures (LNs) of the commercial ferroelectric  $\text{Pb}(\text{Zr}_{0.53}\text{Ti}_{0.47})\text{O}_3$  (PZT) and the natural ferroic relaxor  $\text{Pb}(\text{Fe}_{0.66}\text{W}_{0.33})\text{O}_3$  (PFW) were also fabricated with periodicity of PZT/PFW/PZT ( $\sim 5/1/5\text{ nm}$ , thickness  $\sim 250\text{ nm}$ ) on  $\text{MgO}$  substrate with high remanent polarization ( $P_r$ ) of about  $33\text{ }\mu\text{C/cm}^2$  and magnetization of  $5.32\text{ emu/cc}$  as shown in figure 23. Very low leakage current densities were obtained  $\sim 10^{-7} - 10^{-5}\text{ A/cm}^2$  over  $500\text{ kV/cm}$ . Low leakage current densities, high ferroelectric polarization, well saturated ferromagnetic hysteresis, and flat dielectric constant over wide range of temperature make LNs a potential candidate for artificially designed multiferroics

#### 4. Novel High- $k$ gate oxides for Logic Devices

##### 4.1. High-temperature phase transitions in $\text{SrHfO}_3$ : A Raman scattering study

$\text{SrHfO}_3$  (SHO) is probably the leading gate oxide for the Si chip industry. The material is processed at  $\sim 400\text{K}$  and annealed at high temperature  $\sim 1600\text{ K}$ . Unfortunately, there are two phase transitions in  $\text{SrHfO}_3$  in this temperature range, which can affect the quality of the final films processed, especially their channel mobility in SHO-based n-FET. To clarify these transitions and their impact on  $\text{SrHfO}_3$  processing, we report the temperature dependence of soft phonon modes by Raman spectroscopy. The  $1023\text{K}$  Cmcm-I4mcm transition is found to be displacive (no disorder) and nearly second order. Significant effects are also seen in the orthorhombicorthorhombic Pnma-Cmcm transition at  $670\text{ K}$ .

##### 4.2. Structural phase transition in ternary dielectric $\text{SmGdO}_3$

High-pressure synchrotron based angle dispersive x-ray diffraction (ADXRD) studies were carried out on  $\text{SmGdO}_3$  (SGO) up to  $25.7\text{ GPa}$  at room temperature. ADXRD results indicated a reversible pressure-induced phase transition from ambient monoclinic to hexagonal phase at  $\sim 8.9\text{ GPa}$ . The observed pressure-volume data were fitted

with the third order Birch-Murnaghan equation of state yielding zero pressure bulk modulus  $B_0 = 132(22)$  and  $177(9)$  GPa for monoclinic (B-type) and hexagonal (A-type) phases, respectively. Pressure dependent micro-Raman spectroscopy further confirmed the monoclinic to hexagonal phase transition at about 5.24 GPa. The mode Grüneisen parameters and pressure coefficients for different Raman modes corresponding to each individual phases of SGO were calculated using pressure dependent Raman mode analysis.

#### 4.3. Holmium hafnate: An emerging electronic device material

We have studied structural, optical, charge transport, and temperature properties as well as the frequency dependence of the dielectric constant of  $\text{Ho}_2\text{Hf}_2\text{O}_7$  (HHO) which make this material desirable as an alternative high-k dielectric for future silicon technology devices. A high dielectric constant of  $\sim 20$  and very low dielectric loss of  $\sim 0.1\%$  are temperature and voltage independent at 100 kHz near ambient conditions. The Pt/HHO/Pt capacitor exhibits exceptionally low Schottky emissionbased leakage currents. In combination with the large observed bandgap  $E_g$  of 5.6 eV, determined by diffuse reflectance spectroscopy, our results reveal fundamental physics and materials science of the HHO metal oxide and its potential application as a high-k dielectric for the next generation of complementary metal-oxide-semiconductor devices.

#### 4.4 Optical and band alignment of amorphous zirconium modified $\text{Bi}_{2/3}\text{Nb}_{4/3}\text{O}_7$ thin films on Si

We have investigated optical and band alignment properties of pulsed laser deposited amorphous thin films of bismuth based monoclinic pyrochlore  $\text{Bi}_{2}\text{Zn}_{2/3-x/3}\text{Nb}_{4/3-2x/3}\text{Zr}_x\text{O}_7$  (Zr-BZN) where  $x=0.4$  on quartz and silicon substrates, respectively. The optical parameters, such as complex refractive index ( $n - jk$ ), energy bandgap ( $E_g$ ), complex dielectric function ( $\varepsilon' - j\varepsilon''$ ), and complex conductivity ( $\sigma' - j\sigma''$ ) and associated dispersion parameters were estimated from the UV-Visible transmission spectra. The analysis of refractive index dispersion confirmed the Wemple–Di Domenico single-effective-oscillator model for the direct inter-band transition. The valence band of Zr-BZN is found to be  $\sim 0.1$  eV above that of silicon. The numerical values for conduction band offset  $\Delta E_C$  on silicon and optical bandgap  $E_g$  were estimated to be  $\sim 2.46$  eV and  $\sim 3.46$  eV, respectively for Zr-BZN samples. We determined a complete electron band offset dominated type II staggered band lineup of this high-k dielectric/semiconductor heterostructure, where a straight forward spatial confinement of electrons and holes is facilitated. These important results can play critical role and provide key insight for the practical applications of Zr-BZN material, especially in CMOS (complementary metal-oxide-semiconductor) logic and memory devices.

#### 4.5 Advanced high-k gate dielectric amorphous $\text{LaGdO}_3$ gated metal-oxide-semiconductor devices

Planar metal-insulator-metal (MIM) mono-dielectric layer stacks were fabricated using pulsed laser deposited thin films of high-k dielectric  $\text{LaGdO}_3$  (LGO). These stacks showed high capacitance density  $\sim 43.5$  fF/ $\mu\text{m}^2$  with sub-nanometer capacitance equivalent thicknesses of  $\sim 6.6$  Å, large breakdown field of  $\sim 6.4$  MV/cm, greater energy storage density of  $\sim 40$  J/cm<sup>3</sup>, smaller voltage coefficient of capacitance (VCC), and lower dependence of it on layer thickness ( $\alpha \propto 1/d^{1.07}$ ) and frequency. All these features make LGO a material of interest for next generation MIM structures for radio frequency (RF), analog/mixed-signal (AMS), and dynamic random access memory (DRAM) applications.

### 5. Two Dimensional (2D) Materials

#### 5.1 Cold cathode emission studies on topographically modified $\text{MoS}_2$ films

Nanostructured materials, such as carbon nanotubes, are excellent cold cathode emitters. Here, we report comparative field emission (FE) studies on topographically tailored few layer  $\text{MoS}_2$ films consisting of  $\langle 0001 \rangle$  plane perpendicular ( $\perp$ ) to  $c$ -axis (i.e., edge terminated vertically aligned) along with planar few layer and monolayer (1L)  $\text{MoS}_2$ films. FE measurements exhibited lower turn-on field  $E_{to}$  (defined as required applied electric field to emit current density of  $10 \mu\text{A}/\text{cm}^2$ )  $\sim 4.5$  V/ $\mu\text{m}$  and higher current density  $\sim 1 \text{ mA}/\text{cm}^2$ , for edge terminated vertically aligned (ETVA)  $\text{MoS}_2$ films. However,  $E_{to}$  magnitude for planar few layer and 1L  $\text{MoS}_2$ films increased further to 5.7 and 11 V/ $\mu\text{m}$ , respectively, with one order decrease in emission current density. The observed differences in emission behavior, particularly for ETVA  $\text{MoS}_2$  is attributed to the high value of geometrical field enhancement factor ( $\beta$ ), found to be  $\sim 1064$ , resulting from the large confinement of localized electric field at edge exposed nano-grains. Emission behavior of planar few layers and 1L  $\text{MoS}_2$ films are explained under a two step emission mechanism. Our

studies suggest that with further tailoring the microstructure of ultra thin ETVA MoS<sub>2</sub> films would result in elegant FE properties.

### **5.2 Studies on chemical charge doping related optical properties in monolayer WS<sub>2</sub>**

Thermal stability of quasi particles, i.e., exciton and trion, and a strong particle-particle interaction significantly tune the optical properties of atomically thin two dimensional (2D) metal dichalcogenides. The present work addresses the effect of inherent defects upon optical properties of chemical vapor deposition grown 1 L-WS<sub>2</sub> and proposes the use of chemical transfer doping as a reversible and simple method for identification of the type of excess charge in the system. Photoluminescence (PL) studies in pristine 1 L-WS<sub>2</sub> show that an additional band at  $\sim 0.06$  eV below trion ( $X^\pm$ ) PL band was evolved (at low temperature) which was associated to the bound exciton with charged/neutral defect. Using 7,7,8,8-Tetracyanoquinodimethane and 2,2-bis1,3-dithiolylidene as *p* and *n*-type dopants, respectively, we determined that the inherent defects/metal vacancies, which could be due to the presence of Tungsten metal deficiency, contributed in *p*-type nature of the pristine 1 L-WS<sub>2</sub>. Doping of 2D transition metal dichalcogenides materials with organic molecule via the surface charge transfer method is not only a way to provide a handy way to tailor the electronic and optical properties but also can be used as a tool to determine the nature of defects in the material.

### **5.3 Surface Energy Engineering for Tunable Wettability through Controlled Synthesis of MoS<sub>2</sub>**

MoS<sub>2</sub> is an important member of the transition metal dichalcogenides that is emerging as a potential 2D atomically thin layered material for low power electronic and optoelectronic applications. However, for MoS<sub>2</sub> a critical fundamental question of significant importance is how the surface energy and hence the wettability is altered at the nanoscale in particular, the role of crystallinity and orientation. This work reports on the synthesis of large area MoS<sub>2</sub> thin films on insulating substrates (SiO<sub>2</sub>/Si and Al<sub>2</sub>O<sub>3</sub>) with different surface morphology via vapor phase deposition by varying the growth temperatures. The samples were examined using transmission electron microscopy and Raman spectroscopy. From contact angle measurements, it is possible to correlate the wettability with crystallinity at the nanoscale. The specific surface energy for few layers MoS<sub>2</sub> is estimated to be about 46.5 mJ/m<sup>2</sup>. Moreover, a layer thickness-dependent wettability study suggests that the lower the thickness is, the higher the contact angle will be. Our results shed light on the MoS<sub>2</sub>-water interaction that is important for the development of devices based on MoS<sub>2</sub> coated surfaces for microfluidic applications.

## **6. Theoretical Studies**

### **6.1 STT in MTJs asymmetric barriers**

A series of works supported by this grant deals with the investigation of the bias dependence of the charge and spin current in magnetic tunnel junctions (MTJs) with asymmetric barriers. In particular, we investigated the bias dependence of the tunneling magnetoresistance (TMR) in MTJs with asymmetrically modified barriers. Based on the same formalism we also investigated the spin current and the spin transfer torque (STT) in MTJs with asymmetric barriers. This work had a substantial theoretical component. We derived new expressions for both parallel and perpendicular components of STT in MTJs entirely in terms of collinear quantities. This is possible assuming that the barrier is sufficiently thick to prevent multiple scattering. At the same time it is a much more realistic approximation compared to the infinite barrier approximation used previously. It resulted in excellent agreement with exact results even in the presence of resonant tunneling. In addition, we showed that the STT can be expressed in terms of the scattering matrix elements, which gives them a clear physical interpretation. Using this formalism we showed that modifications of the interfaces can qualitatively change STT behavior. It dramatically changes the slope of the parallel STT and makes the perpendicular STT a monotonous function of the bias. For that reason we suggested that interface engineering can be used to control the bias dependence of STT and optimize the performance of STT-based devices.

### **6.2 Novel MTJs with active barriers**

As a continuation of this line of work we extended our formalism to treat MTJs with active barriers exhibiting additional degrees of freedom which could be controlled by external stimuli. In particular we considered MTJs with ferroelectric (FE) barriers. We predicted that the tunneling electroresistance (TER) effect is present at finite bias even in junctions with inversion symmetry. The effect is highly sensitive to the relative magnetization orientation in the electrodes. We also demonstrated control of the bias dependence of TMR via switching of the ferroelectric

polarization of the barrier. Additionally, we predicted electric-field control of the STT in these junctions. We demonstrated that the bias dependence of the in-plane and out-of-plane components of the STT can be dramatically modified by the ferroelectric polarization. The magnitude of the STT can be enhanced or suppressed by switching the polarization direction and in some cases the sign of STT can be toggled.

Furthermore, we considered MTJs with magnetoelectric antiferromagnetic barriers. In these junctions we predicted a magnetoelectric tunneling electroresistance (ME-TER) effect which is a substantial change of the resistance of the junction in response to switching of the antiferromagnetic order parameter in the barrier in applied electric field by means of the magnetoelectric coupling. The effect is explained in terms of the switching of the orientations of local magnetizations at the barrier interfaces affecting the spin-dependent interface transmission probabilities. Magnetoelectric multiferroic materials with finite ferroelectric polarization exhibit an enhanced resistive change due to polarization-induced spin-dependent screening. These results suggest that devices with active barriers based on single-phase magnetoelectric antiferromagnets represent an alternative nonvolatile memory concept.

### **6.3 Bias dependence of tunneling magnetoresistance (TMR) in magnetic tunnel junctions (MTJs) with asymmetrically modified barriers:**

In collaboration with researchers in SPINTEC, Grenoble, France we investigated the bias dependence of tunneling magnetoresistance (TMR) in magnetic tunnel junctions (MTJs) with asymmetrically modified barriers. Base on model calculations we interpreted experimental observations of asymmetric bias dependence of TMR and a reversal of its sign at large bias in Fe/MgO based MTJs with oxidized interfaces. Our model predicts that this behavior is common to all MTJs with asymmetrically modified barriers. We predict the existence of two distinct TMR regimes: (i) tunneling regime when the interface is modified with layers of a different insulator and (ii) resonant regime when thin metallic layers are inserted at the interface. In the tunneling regime negative TMR is due to the high voltage which overcomes the exchange splitting in the electrodes, while the asymmetric bias dependence of TMR is due to the interface transmission probabilities. In the resonant regime the alignment of the resonance levels with the Fermi surfaces of the electrodes can dramatically change the shape of the TMR bias dependence, including inversion of TMR at zero voltage TMR changing sign with bias.

### **6.3 Formation and properties of the 2-D electron gas at ZnO/Zn(Mg)O (0001) interfaces**

We have studied the formation and properties of the two-dimensional electron gas (2DEG) at ZnO/Zn(Mg)O (0001) interfaces. The mechanism for the 2DEG formation in this system is the spontaneous polarization discontinuity at the interface between the two materials. Polarization discontinuity produces bound charges at the interfaces and correspondingly a confining electric field. The two different interface terminations of ZnO induce bound charges of opposite sign. Thus both n- and p-type 2DEG can be produced by choosing the appropriate interface termination. This system is of interest because of the possibility to dope ZnO with transition metals to produce a room-temperature dilute magnetic semiconductor (DMS). In that case the 2DEG could become spin polarized in addition to displaying high carrier mobility and strong confinement. Uncompensated bound charges at the interface give rise to an electric field in the bulk of ZnO which confines free carriers close to the interface leading to the formation of the 2DEG.

### **6.4 Electric-field-induced magnetization changes in Co/Al<sub>2</sub>O<sub>3</sub> granular multilayers**

We collaborated with an experimental group in the National University of Singapore to study the effect of electric field in the magnetization of Co granules embedded in Al<sub>2</sub>O<sub>3</sub>. Two distinct regimes were observed: (a) low-field regime when the net magnetization of the system changes in a reversible way with the applied electric field and (b) high-field regime when the magnetization decreases irreversibly. Based on model and first-principles calculations we concluded that the first is due to charging and discharging of the granules, while the second is associated with O migration into the granules. The changes in the magnetization of the Co granules are attributed to changes in the position of the Fermi level relative to the minority and majority bands. A higher electric field (~4mV/nm) decreases the magnetization of the granules in an irreversible way. The magnetic moment decrease is attributed to oxidation of Co granules, which is consistent with our first-principles calculations. Our work opens up the possibility to control the magnetization by electrical fields in magnetic granular systems.

### **6.5 Exchange resonance in MDM nanolayer systems: Experiment and theory:** Exchange resonance spectra of three sandwich devices containing nanolayers of Cr, Mn, Co, Ni, and Eu were recorded at 77 K. We found that these

spectra are significantly different from those obtained earlier for Fe-SiO<sub>2</sub>-Au three-layer nanosandwich device. Detailed theoretical approach was developed to analyze the recorded spectra, g-factor values, and relaxation properties of the spin polarized states in the nanolayers. We found that the g-factor values and spin-lattice relaxation rates may be adequately described by the spin-orbit scattering mechanism. Electric charge density fluctuations may also contribute to spin-lattice relaxation in nanolayers. Second-order effects in the relaxation mechanism were also briefly considered.

## 7.0 Education and Outreach Activities

The education and outreach components of the project were developed and executed under the supervision of the project co-director, Dr. Manuel Gomez during entire duration of the project. He worked with students to develop a coherent lesson/educational module to train High school teachers and undergraduates through summer workshops on the following energy related subjects: the Hydrogen economy and technologies, using a model electric car driven by a fuel cell that runs on Hydrogen and uses a fuel cell; the efficiency of light sources by comparing LED and incandescent light sources and developing an experiment that measure the heat losses using a specially designed calorimeter; discussing and measuring the losses of a motor/generator and transmission line losses using basic principles of physics; discussing the hydrogen based energy economy and analyzing the technical complexities of generating, storing and distributing hydrogen. The Lesson/educational modules will be completed in the month of July of this year and will be tested in a physics course next year, and perfected to be used in a summer workshop for teachers and undergraduate students next summer.

Dr. Gomez, with the assistance of the educational coordinator also trained DOE Posdoc fellows and graduate students to serve as explainers and monitor high school students that served in turn as explainers during demonstrations for NanoDays - two days exhibit that took place in Plaza las Americas, the largest shopping mall in Puerto Rico and the Caribbean, where demonstrations of key concepts and applications in nanoscience were developed and offered by trained high school students of different public schools, undergraduate and graduate students. NanoDays is a national public outreach activity organized by the Nanoscale Informal Science Education Network (NISE). From UPR-Rio Piedras, researchers and their graduate and undergraduate students participated in NanoDays for several years. The objective of Nanodays was to disseminate knowledge and understanding of nanoscience and technology among the general public. The activity was a resounding success with more than 7,400 persons visiting the exhibits each year; the evaluation of the activity was judged as very positive by the visitors, as has been the case in previous years. Moreover, three laboratories at UPR Rio Piedras, hosted one student each from US universities, namely UNL Omaha and Nebraska during summer 2011 and 2012.

At UPR-Mayaguez, Graduate and undergraduate students from mechanical engineering and chemical engineering departments have received hands-on training on the synthesis and characterization of multifunctional nanomaterials, powders and thin films. In particular, the students learnt how to operate and analize the data obtained by X-ray diffraction system, Atomic Force Microscopy, UV-Vis spectrophotometer, fluorometer and magnetometry in a VSM system. Participant students were also trained in the preparation of oral and poster presentations to show and discuss their experimental results in local, national and international conferences (PRISM, Transdisciplinary Research Conference, NANOTECH, MRS, ISIF). From January to April 2012, two high school students from the Vocacional School Pedro Perea Fajardo at Mayaguez, were mentored in the science fair project: "Synthesis of Silver Nanoparticles Using Vitamin C". This work was selected to represent Puerto Rico in the area of General Chemistry in the "*National Competition Intel International Science and Engineering Fair*". (May 2012, Pittsburgh, PA). From January 2013 to present, we have supervised three undergraduate students: two from Chemical Engineering and one from Chemistry). These students developed skills in the synthesis of metals nanoparticles (Co, Ag, and Pd), as well as their corresponding characterization using X-ray diffraction, magnetometry, and spectroscopy techniques. They presented their works in different events in Puerto Rico like XVII Sigma Xi Student Poster Day, (April, 2012, Mayaguez PR); JTM/PRISM 2012 Meeting (March 2012, Carolina, PR); 5<sup>th</sup> NEA Science Day (October 2012, Mayaguez, PR). 36<sup>th</sup> Senior Technical Meeting (December 2012, Ponce, PR). 6<sup>th</sup> NEA Science Day (February 2012, Mayaguez, PR). JTM/PRISM 2013 Meeting (March 2012, Caguas, PR). Researchers at UPR Mayaguez, also participated in the demonstration activities like Nanodays (March 2013, Mayaguez PR) for general public.

At UPR- Cayey, a workshop on scanning electron microscopy and nanotechnology was organized for 20 students. Mentored a high school student in summer 2013 to learn about the synthesis of ZnO fibers using the electrospinning technique.

## Published Articles: (Publications with acknowledgement to the DOE-EPSCoR grant)

1. Improved thermal stability and narrowed line width of photoluminescence from InGaN nanorod by ytterbium doping, J. Wang, K. Dasari, K. Cooper, V.R. Thota, J. Wright, R. Palai, D.C. Ingram, E.A. Stinaff, S. Kaya, and W.M. Jadwisienczak, *Phys. Stat. Solidi C* **12**, 413-417 (2015). **Acknowledgements:** WMJ acknowledges the support from the National Science Foundation (NSF) CAREER Award No. DMR-1056493. The work at UPR is supported by the DoE grant DE-FG02-08ER46526. RP thanks NSF CREST Supplement (NSU-UPR) for summer support. We thank A. K. Pradhan and M. Guinel for their experimental help for doing microscopy.
2. Effect of thickness on dielectric, ferroelectric, and optical properties of Ni substituted  $Pb(Zr_{0.2}Ti_{0.8})O_3$  thin films, S. Kumari, N. Ortega, D. K. Pradhan, A. Kumar, J. F. Scott, and R. S. Katiyar, *Journal of Applied Physics*, **118**, 184103 (2015). **Acknowledgments:** This work was supported by NSF Grant EPS-01002410. N. Ortega acknowledges support from the DoE Grant DE-FG02-08ER46526.
3. Studies of phase transitions and magnetoelectric coupling in PFN-CZFO multiferroic composites, Dhiren K. Pradhan, V. S. Puli, S. Kumari, S. Sahoo, P. T. Das, K. Pradhan, Dillip K. Pradhan, J. F. Scott, and R. S. Katiyar, *Journal of Physical Chemistry C*, **120**, 1936 (2016). **Acknowledgment:** This work was supported by DOE Grant No. FG02-08ER46526. D.K.P. and S.K. acknowledge IFN (NSF Grant No. EPS-01002410) for fellowship. We are very much thankful to Prof. R. Palai of University of Puerto Rico for providing magneto-dielectric measurement facilities and Dr. C. V. Rao for FESEM measurements.
4. Nonpolar resistive memory switching with all four possible resistive switching modes in amorphous ternary rare-earth  $LaHoO_3$  thin films, Y. Sharma, S. P. Pavunny, E. Fachini, J. F. Scott, and R. S. Katiyar, *J. Appl. Phys.* **118**, 094506 (2015). **Acknowledgement:** Financial support from DOE Grant No. DE-FG02-08ER46526 is acknowledged. Y. S. is grateful to IFN for graduate fellowship under NSF-RII-0701525 grant. S.P.P. thanks NSF for financial assistance under Grant No: NSF-EFRI RESTOR # 1038272. The authors are thankful to Mr. Oscar Resto for FE-SEM measurements.
5. Optical properties and electronic band lineup on Si of amorphous zirconium modified  $Bi_{2}Zn_{2/3}Nb_{4/3}O_7$  thin films, S. Kooriyattil, S. P. Pavunny, E. Fachini, and R. S. Katiyar, *Journal of Alloys and Compounds*, **644**, 545 (2015). **Acknowledgements:** This work was supported by DOE Grant# DE-FG02-08ER46526. S. K. acknowledges UGC for a Raman fellowship under Indo-US 21<sup>st</sup> century knowledge initiatives [No:5-53/2013(I.C)]. S. P. P. is grateful to NSF for financial assistance under Grant No: NSF-EFRI RESTOR # 1038272.
6. The thermal stability of voltage tunability in pulsed laser deposited  $Ba_{0.6}Sr_{0.4}TiO_3$  thin films, S Kooriyattil, SP Pavunny, AA Instan, RS Katiyar, *Integrated Ferroelectrics* **166** (1), 140-149 (2015). **Acknowledgements:** Financial support from DOE under the grant # DE-FG02-08ER46526 is gratefully acknowledged. S.K. is thankful to UGC, India for a Raman fellowship under Indo-US 21st century knowledge initiatives [No. 5-53/2013(I.C)]. S. P. P. is thankful to IFN for post-doctoral fellowship under NSF grant #1002410.
7. Switchable photovoltaic and polarization modulated rectification in Si-integrated  $Pt/(Bi_{0.9}Sm_{0.1})(Fe_{0.97}Hf_{0.03})O_3/LaNiO_3$  heterostructures, R. Agarwal, Y. Sharma and R. S. Katiyar, *Appl. Phys. Lett.* **107**, 162904 (2015). **Acknowledgements:** This work was supported by the DOE EPSCoR Grant No. DE-FG02-08ER46526. R.A. and Y.S. acknowledge the graduate fellowships received from NSF-IFN Grant No. 1002410.
8. Enhanced resistive switching in forming free graphene oxide films embedded with gold nanoparticles deposited by electrophoresis, G. Khurana, P. Misra, N. Kumar, S. Kooriyattil, J. F. Scott, and R. S. Katiyar, *Nanotechnology* **27**, 015702 (2016). **Acknowledgments:** GK acknowledges the NSF Grant EPS-01002410 for graduate fellowship. The research was supported by the DOE Grant DE-FG02-ER46526. The authors thank Mr. Josue Ortiz, Material Characterizations Center (MCC) UPR, for carrying out XPS measurements.
9. Multifunctional magnetoelectric materials for device applications, N. Ortega, A. Kumar, J. F. Scott, and R. S. Katiyar, *Journal of Physics: Condensed Matter* **27**, 504002 (2015). **Acknowledgments:** This work was supported by the Department of Defense (DoD) W911MF-11-1-0204, grant for release time and materials purchases. N Ortega acknowledges support from the Department of Energy (DoE)-DE-FG02-08ER46526 grant.
10. Graphitic carbon nanospheres: A Raman spectroscopic investigation of thermal conductivity and morphological evolution by pulsed laser irradiation, R. Agarwal, S. Sahoo, V. R. Chitturi, and R. S. Katiyar,

Journal of Applied Physics **118** (21), 214301(2015). **Acknowledgments:** The authors acknowledge financial support from DOE (Grant No. DE-FG02-ER46526). We also acknowledge IFNNSF Grant No. 1002410 for a graduate fellowship (to R.A.) and the post-doctoral fellowship (to S.S.). We thank Mr. Oscar Resto for his help in TEM measurements.

11. Cold cathode emission studies on topographically modified few layer and single layer MoS<sub>2</sub> films, A.P.S. Gaur, S. Sahoo, F. Mendoza, A. M. Rivera, M. Kumar, S. P. Dash, G. Morell, and R. S. Katiyar, *Applied Physics Letters* **108** (4), 043103 (2016). **Acknowledgments:** A.P.S.G. and R.S.K. acknowledge the financial support from the DOE (Grant No. DEG02-ER46526). A.M.R. acknowledges the NSF (Grant No. 0841338). We also acknowledge the NSF for financial support (Cooperative Agreement No. EPS-01002410). We thank Mr. D. Barrionuevo for AFM measurements, and Dr. M. Ahmadi and Dr. M. Guinel for TEM work. We thank Dr. T. Som, Institute of Physics, Bhubaneswar, India, for extending his support to carry out the KPFM measurements.
12. Enhanced tunneling electroresistance in Pt/PZT/ LSMO ferroelectric tunnel junctions in presence of magnetic field D. Barrionuevo, Le Zhang, N. Ortega, A. Sokolov, A. Kumar, J. F. Scott & R. S. Katiyar, *Integrated Ferroelectrics*, **174**, 174 (2016). **Acknowledgments:** This work was supported by IFN-NSF Grant NSF-RII-1002410. N. Ortega is grateful to DOE for financial assistance under DE-FGD2-08ER46526 grant. A. Sokolov and Le Zhang were supported through Materials Research Science and Engineering Center (NSF Grant No. 0820521) and NSF DMR No. 1310542.
13. Influence of growth conditions on the physical properties of Mn doped ZnO thin films grown by reactive magnetron sputtering, Adrián Camacho-Berrios, Víctor Pantojas and Wilfredo Otaño, *MRS proceedings* vol.1805 (2015). DOI: <http://dx.doi.org/10.1557/opr.2015.685>. **Acknowledgments:** The authors would like to thanks Dr. Ram Katiyar and his group from the University of Puerto Rico for the VSM measurements. This work was supported by DOE DE-FG02-08ER46526 and the participation of Adrian Camacho-Berrios was partially supported by NASA Training Grant NNX10AM80H (PR Space Grant). We thank Annemarie Exarhos and Jay Kikkawa at the University of Pennsylvania for facilitating our SQUID measurements, and acknowledge use of the Property Measurement Shared Equipment Facility under NSF DMR-1120901.
14. Visible photoluminescence and room temperature ferromagnetism in high In-content InGaN:Yb nanorods grown by molecular beam epitaxy, K. Dasari, J. Wang, M. J-F Guinel, W.M. Jadwiszczak, H. Huhtinen, R. Mundle, A.K. Pradhan, R. Palai, *J. Appl. Phys.* **118**, 125707 (2015). **Acknowledgements:** The work at University of Puerto Rico was supported by National Science Foundation (DMR-1410869) and the work conducted at Ohio University was sponsored by the National Science Foundation CAREER Award under Contract No. DMR-1056493. R.P. thanks NSF CREST Supplement Award through the Norfolk State University. K.D. thanks Institute for Functional Nanomaterials, UPR for his fellowship.
15. Studies on chemical charge doping related optical properties in monolayer WS<sub>2</sub>, Adriana M. Rivera, Anand P. S. Gaur, Satyaprakash Sahoo, and Ram S. Katiyar, *J. Appl. Phys.* **120**, 105102 (2016). **Acknowledgements:** The authors acknowledge financial support from DOE EPSCOR Project (Grant No. DEG02-ER46526). Dr. S.S. acknowledges NSF Grant No. EPS-01002410 for Post Doctoral Fellowship.
16. Magnetoelectric coupling effect in transition metal modified polycrystalline BiFeO<sub>3</sub> thin films. *Journal of Magnetism and Magnetic Materials.* 369, 9 (2014). DOI: 10.1016/j.jmmm.2014.05.050. **Acknowledgements:** This work was supported by the DOD Grant no.W911NF-11-1- 0204. Acknowledgment is also due to DOE Grant no.FG02-08ER46526 forproviding financial support to the student Dhiren K. Pradhanand toNSF-EFRI RESTOR no.1038272Grant for supporting Dr.VenkataS.Puli.
17. Growth of Sr<sub>2</sub>FeMoO<sub>6</sub> based tri-layer structure for room temperature magnetoresistive applications, Nitu Kumar, P Misra, R K Kotnala, Anurag Gaur and R S Katiyar. *Integrated Ferroelectrics: An International Journal*, 157:1, 89-94, DOI: 10.1080/10584587.2014.912088. **Acknowledgements:** *One of the authors (NK) gratefully acknowledges the CSIR, India for SRF fellowship to carry out this work as a part of his PhD dissertation atNPL, NewDelhi and NITKurukshestra, India. Funding: Authors would like to acknowledge DE-FG02-08ER46526 grant for financial support.*
18. Studies on structural, dielectric, and transport properties of Ni<sub>0.65</sub>Zn<sub>0.35</sub>Fe<sub>2</sub>O<sub>4</sub>. Dhiren K. Pradhan, Pankaj Misra, Venkata S. Puli, Satyaprakash Sahoo, Dillip K. Pradhan and Ram S. Katiyar. *J. Appl. Phys.* **115**, 243904 (2014); <http://dx.doi.org/10.1063/1.4885420>.**Acknowledgements:** *This work was supported by the DOD Grant No.#W911NF-11-1-0204. Acknowledgement is also due to DOE Grant No. # FG02-08ER46526 for providing financial support to Dr. Satyaprakash Sahoo. One of the authors (Dr.P. Misra) acknowledges IFN (Grant No. NSF-RII-0701525) for fellowship. Dhiren K. Pradhan acknowledges IFN (NSF Grant # EPS - 01002410) for fellowship.*
19. High-temperature phase transitions in SrHfO<sub>3</sub>: A Raman scattering study. Manoj K. Singh, Gulab Singh, Tae Hyun Kim, Seiji Kojima, Ram S. Katiyar and J. F. Scott. *Europhysics Letters.* **107** (2), 26004 (2014).

doi:10.1209/0295-5075/107/26004. **Acknowledgements:** MKS and GS are grateful to UGC India for financial support under the major research project (grant No. 39-869/2010). This work was partially supported by the DOE Grant No. DE-FGD2-08ER46526. MKS acknowledges the INSA Delhi and Japan Society for the Promotion of Science (JSPS) for the financial support of his stay at University of Tsukuba, Japan.

20. Surface Energy Engineering for Tunable Wettability through Controlled Synthesis of MoS<sub>2</sub>. Anand P.S. Gaur, Satyaprakash Sahoo, Majid Ahmadi, Saroj P Dash, Maxime J-F Guinel and Ram S. Katiyar. *Nano Lett.*, 2014, 14 (8), pp 4314–4321 (2014). DOI: 10.1021/nl501106v. **Acknowledgements:** The authors acknowledge the financial support from DOE (Grant DE-FG02-ER46526). Anand Gaur acknowledges NSF (fellowship EPS-01002410). We thank Dr. Esteban Fachini and the Materials Characterization Center at UPR for the XPS measurements. We also thank Professor J. F. Scott (University of Cambridge, U.K.) for discussions and NSF for its support (award 0701525) to the Nanoscopy Facility, an electron microscopy facility at UPR.
21. Unipolar resistive switching behavior of amorphous YCrO<sub>3</sub> films for nonvolatile memory applications. Yogesh Sharma, Pankaj Misra, and Ram S. Katiyar. *Journal of Applied Physics* **116**, 084505 (2014); <http://dx.doi.org/10.1063/1.4893661>. **Acknowledgements:** Financial support from DOE Grant No. DE-FG02-08ER46526 is acknowledged. Mr. Y. Sharma and Dr. P. Misra are grateful to IFN for fellowship under NSF-RII-0701525 grant. The authors are thankful to Dr. E. Fachini for useful discussions and helping in conducting XPS experiments.
22. Magnetic structure and interaction in (Sb,Co) co-doped ZnO thin films. K. Samanta, M Sardar, S P Singh and R S Katiyar. *J. Phys. D: Appl. Phys.* **47**, 415003 (2014). **Acknowledgements:** The major part of this work was supported by DOE grant DEFG02-08ER46526. KS also acknowledges encouragement and support by the NPL Director to complete the work.
23. Photovoltaic effect and enhanced magnetization in 0.9(BiFeO<sub>3</sub>)–0.1(YCrO<sub>3</sub>) composite thin film fabricated using sequential pulsed laser deposition. Yogesh Sharma, Pankaj Misra, Rajesh K Katiyar and Ram S Katiyar. *J. Phys. D: Appl. Phys.* **47** 425303 (2014) doi:10.1088/0022-3727/47/42/425303. **Acknowledgements:** Financial support from DOE Grant No DE-FG02-08ER46526 is acknowledged. Authors are grateful to IFN for fellowship under NSF-RII-0701525 grant.
24. Optical, ferroelectric, and piezoresponse force microscopy studies of pulsed laser deposited Aurivillius Bi<sub>5</sub>FeTi<sub>3</sub>O<sub>15</sub> thin films. Sudheendran Kooriyattil, Shojan P. Pavunny, Danilo Barrionuevo and Ram S. Katiyar, *J. Appl. Phys.* **116**, 144101 (2014). <http://dx.doi.org/10.1063/1.4897556>. **Acknowledgements:** This work was supported by DOE grant (DE-FG02-08ER46526). S.K. acknowledges UGC, India for a Raman fellowship under Indo-US 21st century knowledge initiatives (No.: 5-53/2013(I.C)). D.B. is grateful to NSF-IFN for graduate fellowship from NSF-EPS-1002410 grant.
25. Studies of the switchable photovoltaic effect in co-substituted BiFeO<sub>3</sub> thin films. Rajesh K. Katiyar, Yogesh Sharma, Pankaj Misra, Venkata S. Puli, Satyaprakash Sahoo, Ashok Kumar, James F. Scott, Gerardo Morell, Brad R. Weiner, and Ram S. Katiyar. *Appl. Phys. Lett.* **105**, 172904 (2014). <http://dx.doi.org/10.1063/1.4900755>. **Acknowledgements:** R.K.K. is grateful to doctoral fellowship under the NSF Grant No. EPS1002410. Y.S., S.S., and P.M acknowledge financial support from DOE EPSCoR Grant No. DE-FG02-08ER46526.
26. Tunneling Electroresistance in Multiferroic Heterostructures. D. Barrionuevo, Le Zhang, N. Ortega, A. Sokolov, A. Kumar, Pankaj Misra, J. F. Scott, R. S. Katiyar. *Nanotechnology* **25**, 495203 (2014). doi:10.1088/0957-4444/25/49/495203; *Nanotechweb: Tunnelling electroresistance in multiferroic heterostructures*. <http://nanotechweb.org/cws/article/lab/59626>. **Acknowledgements:** This work was supported by the DOE grant (No. DE-FGD2-08ER46526). N Ortega and P Misra are grateful to IFN for financial assistance under NSF-RII-0701525 grant. A Sokolov and Le Zhang were supported through Materials Research Science and Engineering Center (NSF Grant No. 0820521) and NSF DMR No. 1310542.
27. Structural phase transition of ternary dielectric SmGdO<sub>3</sub>: Evidence from angle dispersive x-ray diffraction and Raman spectroscopic studies. Yogesh Sharma, Satyaprakash Sahoo, A. K. Mishra, Pankaj Misra, Shojan P. Pavunny, Abhilash Dwivedi, S. M. Sharma, and Ram S. Katiyar. *Journal of Applied Physics* **117**, 094101 (2015). <http://dx.doi.org/10.1063/1.4913776>. **Acknowledgements:** Financial support from DOE Grant No. DE-FG02-08ER46526 was acknowledged. Y.S. is grateful to IFN for summer fellowship under Grant No. NSF-RII-0701525.
28. Dielectric Anomalies due to Grain Boundary Conduction in Chemically Substituted BiFeO<sub>3</sub>. Shalini Kumari, N. Ortega, A. Kumar, S. P. Pavunny, Jeremiah W. Hubbard, C. Rinaldi, G. Sreenivasulu, J. F. Scott, and Ram S. Katiyar. *J. Appl. Phys.* **117**, 114102 (2015); <http://dx.doi.org/10.1063/1.4915110>. **Acknowledgements:** This

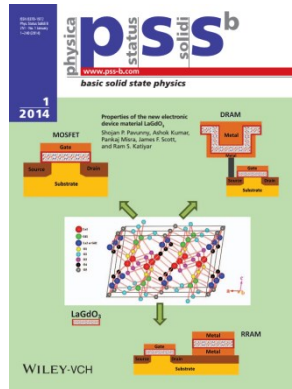
work was supported by the DOE Grant [DE-FG02-08ER46526](#) and NSF (Fellowship EPS 01002410). N.Ortega acknowledges financial support from the NSF-RII Grant R10701525 and Dr. Ashok Kumar was supported by DOD Grant W911NF-11-1-0204. The authors thank JosueOrtiz Morales (MCC) for his help in the XPS measurements.

29. Holmium hafnate: An emerging electronic device material, Shojan P. Pavunny, Yogesh Sharma, Sudheendran Kooriyattil, Sita Dugu, Rajesh K. Katiyar, James F Scott, and Ram S. Katiyar, *Appl. Phys. Lett.* **106**, 112902 (2015). **Acknowledgements:** Financial support from DOE Grant No. [DE-FG02-08ER46526](#) is acknowledged. S.P.P. is grateful to NSF for financial assistance under Grant No. NSF-EFRI RESTOR #1038272. Y.S. is thankful to IFN-NSF for doctoral fellowship under NSF-RII-0701525 grant. The authors are thankful to Mr. Oscar Resto and Mr. Salvador Gavalda for their help in conducting HRTEM experiments and diffuse reflectance spectroscopy measurements, respectively.
30. Ferroelectric Capped Magnetization in Multiferroic PZT/LSMO Tunnel Junctions. Ashok Kumar, D. Barrionuevo, Nora Ortega, A Shukla, Santiranjan Shannigrahi, James F Scott, and Ram Katiyar, *Appl. Phys. Lett.* **106**, 132901 (2015). doi: 10.1063/1.4916732. **Acknowledgements:** This work was supported by DOE (No. DE-FGD2-08ER46526) Grant. D.B. acknowledges support from IFNNSF Grant NSF-RII-1002410 for the graduate fellowship.
31. Enhanced photovoltaic properties in graphitic carbon nanospheres networked TiO<sub>2</sub> nanocomposite based dye sensitized solar cell. Radhe Agarwal, Satyaprakash Sahoo, Venkateswara Rao Chitturi, Joseph D Williams, Oscar Resto, Ram S. Katiyar, *Journal of Alloys and Compounds*. (2015) [doi:10.1016/j.jallcom.2015.03.175](#). **Acknowledgements:** This work was partially supported by the NSF Grant # 1002410, and DOE EPSCoR Grant DE-FG02-08ER46526.
32. Lanthanum Gadolinium Oxide: A New Electronic Device Material for CMOS Logic and Memory Devices, Shojan P. Pavunny, James F. Scott, and Ram S. Katiyar, *Materials* 7(4), 2669-2696 (2014). (Review Article). **Acknowledgements:** The financial support by DOE Grant (DE-FG02-08ER46526) is gratefully acknowledged. The work was initiated while one of us (Shojan Pavunny) was an IFN-UPR fellow supported by the NSF Grant (NSF-EPS-1002410).
33. Ferroelectric/Multiferroic Tunnel Junctions for Multifunctional Applications. N. Ortega, Danilo Barrionuevo, A. Kumar, J. F. Scott and Ram S. Katiyar. Wiley Encyclopedia of Electrical and Electronics Engineering. 1-18 (2015). DOI: 10.1002/047134608X.W8245 (Review Article). **Acknowledgements:** This work was supported by the DOE Grant (No. DE-FGD2-08ER46526). D.B acknowledges support from IFN-NSF Grant NSF-RII-1002410 for the graduate fellowship award.
34. D. Barrionuevo, N. Ortega, A. Kumar, R. Chatterjee, J. Scott, and R. S. Katiyar. *J. Appl. Phys.* 114, 234103 (2013). **Acknowledgements:** This work was supported by the DOE grant No. DE-FGD2-08ER46526. N. Ortega is grateful to IFN for financial assistance under NSF-RII-0701525 grant.
35. Lanthanum Gadolinium Oxide: A New Electronic Device Material for CMOS Logic and Memory Devices, Shojan P. Pavunny, James F. Scott, and Ram S. Katiyar, *Materials* **2014**, 7(4), 2669-2696. (Review article). **Acknowledgements:** The financial support by DOE Grant (DE-FG02-08ER46526) is gratefully acknowledged. The work was initiated while one of us (Shojan Pavunny) was an IFN-UPR fellow supported by the NSF Grant (NSF-EPS-1002410).
36. Ferroelectric and Photovoltaic Properties of Transition Metal doped Pb(Zr<sub>0.14</sub>Ti<sub>0.56</sub>Ni<sub>0.30</sub>)O<sub>3-δ</sub> Thin Films, Shalini Kumari, Nora Ortega, Ashok Kumar, J. F. Scott, R. S. Katiyar, AIP ADVANCES4, 037101 (2014). **Acknowledgements:** This work was supported by the DOE grant DE-FG02-08ER46526. N.Ortega acknowledges financial support from the NSF-RII grant R10701525.
37. Magneto-dielectric anomaly in (Bi<sub>0.95</sub>Nd<sub>0.05</sub>)(Fe<sub>0.97</sub>Mn<sub>0.03</sub>)O<sub>3</sub> electroceramics, Shalini Kumari, Nora Ortega, Ashok Kumar, Ram S. Katiyar, MRS Proceedings 1636 (2014). **Acknowledgements:** This work was supported by the DOE grant DE-FG02-08ER46526. Dr Ashok Kumar was paid for his visit to UPR by the DOD grant # DOD-W911NF-11-1-0204.
38. Room temperature multiferroic properties of Pb(Fe<sub>0.5</sub>Nb<sub>0.5</sub>)O<sub>3</sub>–Co<sub>0.65</sub>Zn<sub>0.35</sub>Fe<sub>2</sub>O<sub>4</sub> Composites, Dhiren K. Pradhan, Venkata S. Puli, Satya N. Tripathy, Dillip K. Pradhan, J.F.Scott, and Ram S. Katiyar, *Journal of Applied Physics*, **114**, 234106, (2013). **Acknowledgements:** This work was supported by the DOD grant #W911NF-11-1-0204. Acknowledgement is also due to DOEs grant # FG02-08ER46526 for providing financial support to the student Dhiren K. Pradhan and to NSF-EFRI RESTOR # 1038272 grant for supporting the student Venkata. S. Puli.
39. Studies on magnetoelectric coupling in PFN-NZFO Composite at room temperature, Dhiren K. Pradhan, Satyaprakash Sahoo, Sujit K. Barik, Venkata S. Puli, Pankaj Misra and Ram S. Katiyar, *Journal of Applied*

Physics, **115**, 194105, (2014). **Acknowledgements:** This work was supported by the DOE-DE-FG02-08ER46526 grant. One of the authors (P. Misra) acknowledges IFN (Grant No. NSF-RII-0701525) for fellowship.

40. Properties of the new electronic device material LaGdO<sub>3</sub>, S. P. Pavunny, A. Kumar, P. Misra, J. F. Scott, and R. S. Katiyar, *Phys. Status Solidi B*, **251**, No. 1, 131–139 (2014). DOI 10.1002/pssb.201349257. **Acknowledgements:** The financial support by DOE Grant# DE-FG02-08ER46526 is gratefully acknowledged.

**The relevant picture of the above article has been published on the cover page of the Phys. Status Solidi B. January 2014 issue**



41. Phonons and magnetic excitation correlations in weak ferromagnetic YCrO<sub>3</sub>, Y. Sharma, S. Sahoo, W. Perez, et al. *J. Appl. Phys.* **115**, 183907 (2014). **Acknowledgements:** The authors acknowledge financial support from DOE (Grant No. DE-FG02-ER46526) and Department of Science and Technology (Grant No. SB/S3/ME/29/2013), India.

42. Forming Free Resistive Switching in Graphene Oxide Thin Film for Thermally Stable Nonvolatile Memory Applications, Geetika Khurana, Pankaj Misra and Ram S. Katiyar, *J. Appl. Phys.* **114**, 124508 (2013). **Acknowledgements:** Authors would like to acknowledge DE-FG02-08ER46526 Grant for financial support.

43. Multilevel resistive memory switching in graphene sandwiched organic polymer heterostructure, Geetika Khurana, Pankaj Misra and Ram S. Katiyar, *Carbon*, doi.org/10.1016/j.carbon.2014.04.085, (2014) **Acknowledgements:** The authors acknowledge financial support from DOE- United States (Grant No. DE-FG02-ER46526). One of the authors (P. Misra) acknowledges IFN (Grant No. NSF-RII-0701525) for fellowship.

44. Optical and Vibrational Studies of Partially Edge-Terminated Vertically Aligned Nanocrystalline MoS<sub>2</sub> Thin Films, Anand PS Gaur, Satyaprakash Sahoo, Majid Ahmadi, Maxime J-F Guinel, Sanjeev K Gupta, Ravindra Pandey, Sandwip K Dey, Ram S Katiyar, *J. Phys. Chem. C* **2013**, **117**, 26262–26268. **Acknowledgements:** The authors acknowledge financial support from the U.S. Department of Energy (DOE) (Grant DE-FG02-08ER46526). A. P. S. Gaur is thankful for the National Science Foundation (NSF) fellowship (Grant NSF-RII-1002410).

45. Optical studies and crystal field calculation of GaN nanorods doped with Yb<sup>3+</sup> ions, T. Kallel, M. Dammak, J. Wang, W. M. Jadwisienczak, J. Wu, and R. Palai, *Journal of Alloys and Compounds*, **609**, 284-289 (2014). **Acknowledgements:** The work conducted at Ohio University was supported by the NSF CAREER Award No DMR-1056493. The work at the University of Puerto Rico was supported by DoE-EPSCoR (#DE-FG02-08ER46526).

46. Quantum Filter of Spin Polarized States: Metal - Dielectric - Ferromagnetic/Semiconductor Device, V. I. Makarov, I.V. Khmelinskii, Manuscript was accepted November 15, 2013, *Material Research Bulletin*, **50**, 2014, **3**, 514-523. **Acknowledgement:** V.M. is very grateful for financial support from Grant #DE-F602-08ER46526 from DOE.

47. Intrinsic noise from neighboring bases in the DNA transverse tunneling current, J. R. Alvarez, D. Skachkov, S. E. Massey, J. Lu, A. Kalitsov, and J. P. Velev, *Physical Review Applied* **1**, 034001 (2014). **Acknowledgements:** This work was supported by the National Science Foundation (Grants No. EPS-1002410, No. EPS-1010094, and No. DMR-1105474) and the U.S. Department of Energy (Grant No. DE-FG02-08ER46526).

48. Bias dependence of tunneling magnetoresistance in magnetic tunnel junctions with asymmetric barriers, A. Kalitsov, P.-J. Zermatten, F. Bonell, G. Gaudin, S. Andrieu, C. Tiusan, M. Chshiev, and J. Velev, *Journal of Physics: Condensed Matter* **25**, 496005 (2013). **Acknowledgements:** The work at the University of Puerto Rico

was supported by NSF (Grants Nos EPS-1002410, EPS-1010094, and DMR- 1105474) and DOE (Grant No. DE-FG02-08ER46526). P-J Zermatten, G Gaudin, F Bonell, S Andrieu, and C Tiusan acknowledge the SPINCHAT project ANR-07-BLAN-341. C Tiusan acknowledges POS CCE ID. 574, code SMIS-CSNR 12467.

49. Spin torque in magnetic tunnel junctions with asymmetric barriers, A. Kalitsov, W. Silvestre, M. Chshiev, and J. Velev, , Physical Review B 88, 104430 (2013). **Acknowledgements:** A.K. and J.V. thank N. Kioussis for the useful discussions. This paper was supported by the National Science Foundation (NSF, Grants No. EPS-1002410 for A.K. and No. DMR- 1105474 for W.S.), the U.S. Department of Energy (Grant No. DE-FG02-08ER46526 for J.P.V.), and the French National Center of Scientific Research. Computations were performed at the high-performance computing facility at the University of Puerto Rico supported by the NSF (Grant No. EPS-1010094).
50. Polarization discontinuity induced two-dimensional electron gas at ZnO/Zn(Mg)O interfaces: A first-principles study, J. Betancourt, J. Saavedra, J. D. Burton, Y. Ishikawa, E. Tsymbal, and J. Velev, Physical Review B 88, 085418 (2013). **Acknowledgements:** This work was supported by the National Science Foundation through Nebraska and Puerto-Rico EPSCOR (Grants Nos EPS-1010674, EPS-1002410 and EPS-1010094), Nebraska MRSEC (Grant No. DMR-0820521) and DMR (Grant No. DMR-1105474), and the Department of Energy (Grant No. DE-FG02-08ER46526).
51. Effect of Current Compliance on Resistive Switching Characteristics of Amorphous Ternary Rare Earth Oxide SmGdO<sub>3</sub> Grown by Pulsed Laser Deposition, Pankaj Misra, Yogesh Sharma and Ram S. Katiyar, ECS Trans. 61 (6), 133-138 (2014). **Acknowledgements:** The authors acknowledge financial support from DOE (grant DE-FG02-ER46526). One of the authors (P. Misra) acknowledges IFN (Grant NSF-EPS-1002410) for fellowship.
52. Enhanced photoresponse in BiFeO<sub>3</sub>/SrRuO<sub>3</sub> heterostructure, Rajesh K. Katiyar, Pankaj Misra, Satyaprakash Sahoo, Gerardo Morell, Ram S. Katiyar, Journal of Alloys and Compounds 609, 168-172 (2014). **Acknowledgements:** This work was supported by the DOE grant DE-FG02-08ER46526. Financial support by the NSF Grant # 1002410 is also acknowledged for providing fellowship to RKK.
53. Polycrystalline Sr<sub>2</sub>FeMoO<sub>6</sub> thin films on Si substrate by pulsed lased deposition for magnetoresistive applications, N. Kumar, P. Misra, R. K. Kotnala, A. Gaur, R. Rawat, R. J. Choudhary, R. S. Katiyar, Materials Letters 118, 200-203 (2014). **Acknowledgements:** The authors acknowledge the financial support from DOE (grant DE-FG02-ER46526). One of the author N. Kumar gratefully acknowledges CSIR, India for SRF fellowship to carry out this work as a part of his Ph.D. dissertation at NPL, New Delhi and NIT Kurukshetra, India.
54. Multilevel unipolar resistive memory switching in amorphous SmGdO<sub>3</sub> thin film, Y. Sharma, P. Misra, S. P. Pavunny, R. S. Katiyar; Applied Physics Letters 104 (7), 073501(2014). **Acknowledgements:** The authors acknowledge financial support from DOE (grant DE-FG02-ER46526).
55. Room temperature magnetoresistance in Sr<sub>2</sub>FeMoO<sub>6</sub>/SrTiO<sub>3</sub>/Sr<sub>2</sub>FeMoO<sub>6</sub> trilayer devices, N. Kumar, P. Misra, RK Kotnala, A Gaur, RS Katiyar, Journal of Physics D: Applied Physics 47 (6), 065006 (2014). **Acknowledgements:** The author N Kumar gratefully acknowledges the CSIR, India for SRF fellowship to carry out this work as a part of his PhD dissertation at NPL, New Delhi and NIT Kurukshetra, India. The authors acknowledge the support from DOE (grant DE-FG02-ER46526) and would like to thank Ms G Khurana of UPRRP for her help taking FESEM and MR micrographs. The authors are also thankful to Dr R J Choudhary of DAE-UGC, Consortium for Scientific Research, Indore India, for magnetic measurements.
56. Structural and Electrical Characteristics of Ternary Oxide SmGdO<sub>3</sub> for Logic and Memory Devices, Y Sharma, P Misra, RS Katiyar; MRS Proceedings Vol. 1633, 129 (2014) **Acknowledgements:** The authors acknowledge financial support from DOE grant DE-FG02-ER46526.
57. Advanced high-k dielectric a-LaGdO<sub>3</sub> based high density MIM capacitors with sub-nanometer capacitance equivalent thickness; S. P. Pavunny, P. Misra, J. F. Scott, and R. S. Katiyar Room Temperature Novel Multiferroic, Appl. Phys. Lett. 102 (25), 252905 (2013). **Acknowledgements:** Financial support from DOE (Grant No. DE-FG02-08ER46526) is acknowledged. S. P. Pavunny and P. Misra are grateful to Institute for Functional Nanomaterials for fellowships under the NSF-RII-1002410 grant.
58. Nonvolatile Resistive Memory Switching in Amorphous LaGdO<sub>3</sub> Thin Films, P Misra, SP Pavunny, RS Katiyar, MRS Proceedings Vol. 1562 (2013). **Acknowledgements:** Authors would like to acknowledge NSF-EPS-1002410 grant for fellowships and DE-FG02-08ER46526 grant for materials expanses.
59. Advanced high-k gate dielectric amorphous LaGdO<sub>3</sub> gated MOS devices with sub-nanometer equivalent oxide thickness; S. P. Pavunny P. Misra, R. Thomas, A. Kumar, J. Schubert, J. F. Scott, and R. S. Katiyar; Appl. Phys. Lett.102 (19), 192904 (2013). **Acknowledgements:** Financial support from DOE Grant No. DE-FG02-

08ER46526 is acknowledged. Mr. S. P. Pavunny and Dr. R. Thomas are grateful to IFN for financial assistance under NSF-RII-0701525 grant.

60. Observation of strong magnetoelectric effects in  $\text{Ba}_{0.7}\text{Sr}_{0.3}\text{TiO}_3/\text{La}_{0.7}\text{Sr}_{0.3}\text{MnO}_3$  thin film heterostructures, R. Martinez, A. Kumar, R. Palai, G. Srinivasan, and R. S. Katiyar, *J. Appl. Phys.* **111**, 104104 (2012). **Acknowledgements:** This work was supported by the US Department of Energy (DoE-EPSCoR) under Grant No. DE-FG02-08ER46526 and the NSF grant DMR-0902701 at Oakland University

61. Room temperature structural, morphological, and enhanced ferroelectromagnetic properties of  $x\text{Ba}_{0.7}\text{Ca}_{0.3}\text{TiO}_3-(1-x)\text{BaFe}_{0.2}\text{Ti}_{0.8}\text{O}_3$  multiferroic composites. V. S. Puli, I. Coondoo, N. Panwar, A. Srinivas, and R. S. Katiyar. *J. Appl. Phys.* **111**, 102802 (2012). **Acknowledgements:** This work was supported by the Department of Energy Grant No. DoE FG 02-08ER46526. Authors would like to thank Cristina Diaz Borrero, Material characterization center, University of Puerto Rico for performing SEM measurements. The authors I.C. and N.P. would like to thank the Portuguese Foundation for Science and Technology through their research grants SFRH/BPD/81032/2011 and SFRH/BPD/71289/2010, respectively.

62. Structural and magnetic properties of N doped ZnO thin films. Kajal Jindal, Monika Tomar, R. S. Katiyar, and Vinay Gupta. *J. App. Phys* **111**, 102805 (2012). **Acknowledgements:** Authors are thankful to Professor C. Jagadish, Australian National University, Australia for the fruitful discussions. This work was supported partially by the Department of Science and Technology, India and DOE Grant No. DEFG02-08ER46526. One of the authors K.J. is also thankful to the UGC and University of Delhi for the research fellowship and teaching assistantship, respectively.

63. Temperature dependent dynamics of ZnO nanoparticles probed by Raman scattering: A big divergence in the functional areas of nanoparticles and bulk materials. Harish Kumar Yadav, R. S. Katiyar, and Vinay Gupta. *Appl. Phys. Lett.* **100**, 051906 (2012). **Acknowledgements:** The authors are thankful to DST, India and the DOE (Grant No. DE - FG02- 8ER46526), USA for financial support.

64. In-plane dielectric and magnetoelectric studies of  $\text{BiFeO}_3$ . Ashok Kumar, J. F. Scott, R. Martinez, G. Srinivasan, and R. S. Katiyar. *Phys. Status Solidi A* **209**, No. 7, 1207–1212 (2012). **Acknowledgements:** This work was partially supported by EPSRC (at Cambridge), W911NF-06-1-0183, W911NF1110204, and DoE FG 02-08ER46526 grants

*One of the Figures corresponding to the above article was chosen as cover of the Phys. Status Solidi A (PSS) and the article was selected to be part of 2013 Edition of “Best of PSS”*

65. Effect of Electrode Resistance on Dielectric and Transport Properties of Multiferroic Superlattice: A Impedance Spectroscopy Study, S. Dussan, A. Kumar, J. F. Scott, and R. S. Katiyar, *AIP Advances*, **2**, 032136 (2012). **Acknowledgements:** This work was partially supported by DoE FG 02-08ER46526 and DoD W911MF-11-1- 0204 grants to UPR. One of the authors S.D. acknowledges an IFN fellowship.

66. Optical Dielectric Function Modeling and Electronic Band Lineup Estimation of Amorphous High-k  $\text{LaGdO}_3$  Films, S. P. Pavunny, R. Thomas, A. Kumar, J. F. Scott, and R. S. Katiyar, *ECS Journal of Solid State Science and Technology*, 1(4) N53-N57 (2012). **Acknowledgements:** Financial support from DOE grant# DE-FG02-08ER46526 is acknowledged. S. P. Pavunny and Dr. R. Thomas are grateful to IFN for financial assistance under NSF-RII-0701525 grant.

67. Relaxor-ferroelectric superlattices: A High energy density capacitor. N. Ortega, A. Kumar, J. F. Scott, Douglas B. Chrisey, M. Tomazawa, Shalini Kumari, D. G. B. Diestra, and R. S. Katiyar. *J. Phys.: Condens. Matter.* **24**, 445901 (2012). **Acknowledgements:** This work was supported by NSF-EFRI-RPI-1038272 grant. One of the authors (N Ortega) is also thankful to the DOE-DE-FG02-08ER46526 for financial support.

68. A New Room-Temperature Multiferroic: Lead iron Tantalate Zirconate Titanate. Dilsom Sanchez, Ashok Kumar, Nora Ortega, R. S. Katiyar, J. F. Scott, R. Roque-Malherbe R. Polanco, *Emerging Materials Research*, **1**, S1, 27-33, (2012). **Acknowledgements:** This work was partially supported by W911NF-11-1-0204, IFN-NSF-RII 07-01-25, and DoE FG 02-08ER46526 grants.

69. Room Temperature Novel Multiferroic Single Phase Material:  $(\text{PbFe}_{0.5}\text{Ta}_{0.5}\text{O}_3)_x-(\text{PbZr}_{0.53}\text{Ti}_{0.47}\text{O}_3)_{(1-x)}$ , D. Sánchez, N. Ortega, R. S. Katiyar ,Ashok Kumar, J.F. Scott, *21 IEEE International Symposium on the Applications of Ferroelectrics (ISAF)* proceeding (2012); doi:[10.1109/ISAF.2012.6297747](https://doi.org/10.1109/ISAF.2012.6297747). **Acknowledgements:** This work is partially supported in parts by DOE-DE-FG02-08ER46526 and DoD W911MF-11-0204 grants.

70. Dielectric and Magnetic properties of  $\text{Pb}(\text{Fe}_{0.5}\text{Nb}_{0.5})\text{O}_3 - \text{Ni}_{0.65}\text{Zn}_{0.35}\text{Fe}_2\text{O}_4$  Composites. Dhiren K. Pradhan, Sujit K. Barik, Venkata S. Puli, Satyaprakash Sahoo, Ram S. Katiyar. *ECS Trans.* **50**, 59-65 (2013). doi: 10.1149/05004.0059ecst. **Acknowledgements:** This work was supported in part by DOE-DE-FG02-08ER46526 and W911NF-11-1-0204 grants.

71. Room-Temperature Single Phase Multiferroic Magnetoelectrics:  $\text{Pb}(\text{Fe, M})_x(\text{Zr,Ti})_{(1-x)}\text{O}_3$  [M = Ta, Nb]. Dilsom A. Sanchez, Nora Ortega, Ashok Kumar, G. Sreenivasulu, Ram S. Katiyar, J. F. Scott, Donald M. Evans, Miryam Arredondo-Arechavala, A. Schilling<sup>5</sup>, and J. M. Gregg. *J. Appl. Phys.* **113**, 074105 (2013). **Acknowledgements:** This work was supported in parts by DOE (DE-FG02-08ER46526), DOD (W911NF-11-1-0204) and NSF (EPS-1002410) grants. D. Sanchez was supported by an IFN-NSF Fellowship, while N. Ortega and A. Kumar were supported by DOE and DOD grants, respectively. The authors thank Frank Mendoza for his help with the FESEM-EDX measurements.

72. Investigations on electrical and magnetic properties of multiferroic  $[(1-x)\text{Pb}(\text{Fe}_{0.5}\text{Nb}_{0.5})\text{O}_3-x\text{Ni}_{0.65}\text{Zn}_{0.35}\text{Fe}_2\text{O}_4]$  composites. Dhiren K. Pradhan, Sujit K. Barik, Venkata S. Puli, Satyaprakash Sahoo, Ram S. Katiyar. *J. Appl. Phys.* **113**, 144104 (2013); <http://dx.doi.org/10.1063/1.4799414>. **Acknowledgements:** This work was supported in part by DOE-DE-FG02-08ER46526 and W911NF-11-1-0204 grants

73. In-situ Raman Studies of Electrically Reduced Graphene Oxide and Its Field Emission Properties, Satyaprakash Sahoo, Geetika Khurana, Sujit Barik, , Sandra Dussan, D. Barrionuevo, Ram S Katiyar. *J. Phys. Chem. C.* **117** (10), pp 5485-5491. (2013). DOI: 10.1021/jp400573w. **Acknowledgements:** We acknowledge partial financial support from DoE through grant no. DE-FG02-ER46526.

74. High-temperature phase transitions in a quaternary lead based perovskite structured materials with Negative temperature coefficient resistor (NTCR) behavior, Ricardo Martínez, Venkata Sreenivas Puli, Ram S. Katiyar, Journal of Materials Science: *J Mater Sci: Mater Electron* (2013). DOI 10.1007/s10854-013-1172-8. **Acknowledgements:** This work was supported by the US Department of Energy (DoE-EPSCoR) under Grant No. DE-FG02-08ER46526. One of the authors (Ricardo Martinez) would like to thank to the Institute for Functional Nanomaterials (IFN) through University of Puerto Rico for support his fellowship.

75. Characteristics of  $\text{BaTiO}_3/(\text{Ba},\text{Sr})\text{TiO}_3$  superlattices synthesized by pulsed laser deposition. Ortega N, Ashok Kumar, J.F. Scott and Ram S. Katiyar. Processing and Properties of Advanced Ceramics and Composites V: Ceramic Transactions, Vol. 240. 293-300 (2013). Edited by: by N. P. Bansal, J. P. Singh, S. Ko, R. Castro, G. Pickrell, N. J. Manjooran, M. Nair, G. Singh. Wiley , ISBN: 978-1-118-74409-3. **Acknowledgements:** This work was partially supported by NSF-EFRI-RPI-1038272 and DOE-DE-FG02-08ER46526 grants.

76. Advanced high-k gate dielectric  $\text{LaGdO}_3$  based MOS devices with sub-nanometer equivalent oxide thickness. S. P. Pavunny, P. Misra, R. Thomas, A. Kumar, J. F. Scott and R. S. Katiyar. *Appl. Phys. Lett.* **102**, 192904 (2013). **Acknowledgements:** Financial support from DOE Grant No. DE-FG02- 08ER46526 is acknowledged. Mr. S. P. Pavunny and Dr. R. Thomas are grateful to IFN for financial assistance under NSF-RII-0701525 grant. The authors are thankful to Mr. O. Resto and Dr. M. Correa for their help in conducting HRTEM experiments and to Professor L. Fonseca for providing the electroding facility.

77. Effect of oxygen on Jahn-Teller distortion and magnetization dynamics in  $\text{Pr}_{0.9}\text{Ca}_{0.1}\text{MnO}_3$  thin films. S. Majumdar, H. Huhtinen, P. Paturi, and R. Palai. *J. Phys.: Condens. Matter*, **25**, 066005 (2013). **Acknowledgements:** The Wihuri Foundation, the Academy of Finland and the Turku Collegium for Science and Medicine (TCSM) are acknowledged for financial support. RP thanks DoE-EPSCoR for financial support.

78. Effect of Praseodymium Species on the Structural and Functional Properties of Nanocrystalline  $\text{BiFeO}_3$  Powders and Thin Films. Gina Montes Albino, Marco Gálvez-Saldaña and Oscar Perales-Pérez. *MRS Proceedings*, **1454**, 39-44 (2012). doi:10.1557/opr.2012.1067. **Acknowledgements:** This material is based upon work supported by the DOE-Grant No FG02-08ER46526. Special thanks to M.S. Boris Renteria, UPRM, for the AFM and magnetic measurements in the NANOmaterials Processing Laboratory at UPRM, and Dr. Ram Katiyar's group for the ferroelectric measurements in the Speclab Laboratory at UPR-Rio Piedras Campus.

79. Ferromagnetism in Nanocrystalline Powders and Thin Films of Cobalt-Vanadium co-doped Zinc Oxide. Marco Gálvez-Saldaña, Gina Montes-Albino and Oscar Perales-Perez *MRS Proceedings*, **1449** mrss12-1449-bb06-15 (2012). doi:10.1557/opr.2012.794. **Acknowledgements:** This material is based upon work supported by the DOE-Grant No FG02-08ER46526. Special thanks to M.S. Boris Rentería, UPRM, for the magnetic measurements at the NANO materials Processing Laboratory at UPRM

80. Effect of the Type of Solvent and Bi-Stoichiometric Excess on the Purity of Nanocrystalline Bismuth Ferrite Single Phase. Gina Montes-Albino, Marco Gálvez-Saldaña, Boris Renteria-Beleño and Oscar Perales-Pérez. *MRS Proceedings*, 1454, 45-50 (2012). doi:10.1557/opr.2012.1232. **Acknowledgements:** *This material is based upon work supported by the DOE-Grant No FG02-08ER46526. Special thanks to Dr. Ram Katiyar, Ventaka Sreenivas Puli, Frank Mendoza and Danilo Barrionuevo from SpecLaboratory at UPR-Rio Piedras Campus for the electric measurements and SEM imaging.*

81. Study on the Structural, Electrical and Magnetic Properties of Pure and (Pr<sup>3+</sup>, Co<sup>2+</sup>)-Doped BiFeO<sub>3</sub> Powders and Thin Films. Gina Montes Albino, Marco Gálvez-Saldaña and Oscar Perales-Pérez. *Jap. J. Appl. Phys.*, 51, 11PG06-1-4 (2012). **Acknowledgements:** *This material is based upon work supported by the DOEGrant No. FG02-08ER46526. Special thanks to Dr. Ram Katiyar's group for the ferroelectric measurements in the Speclab Laboratory at UPR—Rio Piedras Campus.*

82. Electric-field-induced magnetization changes in Co/Al<sub>2</sub>O<sub>3</sub> granular multilayers. Sahadevan, A. Kalitsov, G. Kalon, C. Bhatia, J. Velev, and H. Yang, , *Phys. Rev. B* **87**, 014425 (2013). **Acknowledgements:** *This work was partially supported by the Singapore NRF under CRP Award No. NRF-CRP 4-2008-06, NSF (Grants No. EPS-1002410 and No. EPS-1010094), and Department of Energy (Grant No. DE-FG02-08ER46526).*

83. On the Resistive Switching and Current Conduction Mechanisms of Amorphous LaGdO<sub>3</sub> Films Grown by Pulsed Laser Deposition, P. Misra, S. P. Pavunny and R. S. Katiyar, *ECS Transactions*, 53 (3) 229-235 (2013). **Acknowledgements:** *Authors would like to acknowledge NSF-EPS-1002410 grant for fellowships and DE-FG-02-08ER46526 grant for materials expanses.*

84. Nonvolatile Resistive Memory Switching in Amorphous LaGdO<sub>3</sub> Thin Films; P. Misra, S. P. Pavunny and R. S. Katiyar; *MRS spring meeting proceedings*, manuscrtp ID: 1566531 (2013). **Acknowledgements:** *Authors would like to acknowledge NSF-EPS-1002410 grant for fellowships and DE-FG02- 08ER46526 grant for materials expanses.*

85. Spin-polarized state quantum filter used to measure spin-polarized state relaxation time and g-factor. Vladimir I. Makarov and Igor Khmelinskii. *J. Appl. Phys.* 113, 084304 (2013). <http://dx.doi.org/10.1063/1.4792658>. **Acknowledgements:** *V.M. is very grateful for financial support from Grant #DE-FG02-08ER46526.*

86. Exchange Resonance in MDM Nanolayer Systems: Experiment and Theory. Vladimir I. Makarov, Igor Khmelinskii, *J. Chem. Phys.*, **138**, 074705 2013. **Acknowledgements:** *V.M. is very grateful for financial support from Grant #DE-FG02-08ER46526.*

87. Growth of carbon nanotubes on spontaneously detached free standing diamond films and their field emission properties, Deepak Varshney, Anirudha V Sumant, Brad R. Weiner; Gerardo Morell. *Diamond and Related Materials*, 30, 42-47 (2012), DOI: 10.1016/j.diamond.2012.09.009. **Acknowledgements:** *This research was carried out under the auspices of the Institute for Functional Nanomaterials (NSF Grant 1002410), PR NASA EPSCoR (NASA Cooperative Agreement NNX07AO30A) and PR DOE EPSCoR (DOE Grant DE-FG02-08ER46526)*

88. Temperature-Dependent Raman Studies and Thermal Conductivity of Few-Layer MoS<sub>2</sub>, Satyaprakash Sahoo, Anand P. S. Gaur , Majid Ahmadi , Maxime J.-F. Guinel , and Ram S. Katiyar, *J. Phys. Chem. C*, 117, 9042 (2013). **Acknowledgements:** *We acknowledge partial financial support from NSF-RII-1002410 and DOE through Grant no. DE-FG02-ER46526.*

89. Spontaneously detaching self-standing diamond films, Varshney, Deepak; Kumar, Ashok; Guinel, Maxime J. -F.; Weiner, Brad R.; Morell, Gerardo; *Diamond and Related Materials* 21, 99-31 (2012). DOI:10.1016/j.diamond. 2011.10.024. **Acknowledgements:** *This research was made possible by funds from the Institute for Functional Nanomaterials (NSF Grant # 1002410), PR NASA EPSCoR (NASA Cooperative Agreement # NNX07AO30A and NNX08BA48A), and PR DOE EPSCoR (DOE Grant # DEFG02-08ER46526). We would like to acknowledge the help of Mr. W. Pérez with the Raman spectroscopy measurements.*

90. Atomic and Electronic Properties of Realizable Size Single-Crystal GaN Nanotubes by First Principles, Yilmaz, Hulusi; Singh, Surinder P.; Marin, Carlos; Morell, Gerardo; *Journal of Nanoscience and Nanotechnology*, 11(9) :7753-7761 (2011) DOI:10.1166/jnn.2011.4727. **Acknowledgements:** *This research was made possible by funds from the Institute for Functional Nanomaterials (NSF Grant # 1002410), PR NASA EPSCoR (NASA Cooperative Agreement # NNX07AO30A and NNX08BA48A), and PR DOE EPSCoR (DOE Grant # DEFG02-08ER46526). We would like to acknowledge the help of Mr. W. Pérez with the Raman spectroscopy measurements.*

91. Free standing graphene-diamond hybrid films and their electron emission properties. Varshney, Deepak; Rao, Chitturi Venkateswara; Guinel, Maxime J.-F.; Weiner, Brad R.; Morell, Gerardo; *J. Appl. Phys.* 110, 044324 (2011), DOI: 10.1063/1.3627370. **Acknowledgements:** *This research was made possible by funds from the Institute for Functional Nanomaterials (NSF Grant # 1002410), PR NASA EPSCoR (NASA Cooperative Agreement # NNX07AO30A and NNX08BA48A), and PR DOE EPSCoR (DOE Grant # DEFG02-08ER46526). We would like to acknowledge the help of Mr. W. Pérez for the Raman spectroscopy measurements, the Nanoscopy Facility at UPR for TEM measurements, and the MCC for the SEM image.*
92. Conformal coating of ferroelectric oxides on carbon nanotubes; F. Mendoza, A. Kumar, R. Martínez, J.F. Scott, B. Weiner, R.S. Katiyar, G. Morell; *European Physics Letters* 97, 27001, 2012. **Acknowledgements:** *This research was made possible by funds from the Institute for Functional Nanomaterials (NSF Grant # 1002410), PR NASA EPSCoR (NASA Cooperative Agreement # NNX07AO30A and NNX08BA48A), and PR DOE EPSCoR (DOE Grant # DEFG02-08ER46526). We would like to acknowledge the help of Mr. W. Pérez for the Raman spectroscopy measurements, the Nanoscopy Facility at UPR for TEM measurements, and the MCC for the SEM image.*
93. Multiferroic properties of  $\text{Bi}_{4-x}\text{Nd}_x\text{Ti}_3\text{O}_{12}/\text{CoFe}_2\text{O}_4$  composite Film. D. Barriónuevo, S.P. Singh, and M.S. Tomar, *Integrated ferroelectrics* 124, 48-52 (2011). Acknowledgements: This work was supported by DoE-EPSCoR Grant No. DE-FG02-08ER46526 and is gratefully appreciated.
94. Raman spectroscopy to probe residual stress in  $\text{ZnO}$  nanowire, S. Sahoo. G.L. Sharma, and R. S. Katiyar, *Journal of Raman Spectroscopy*, 43, 72 (2012).
95. Dielectric Properties and Electrical conduction of high-k  $\text{LaGdO}_3$  Ceramics, S. P. Pavunny, R. Thomas, A. Kumar, N. M. Murari, and R. S. Katiyar, *Journal of Applied Physics*, 111, 102811 (2012)
96. Cauchy-Urbach Dielectric Function Modeling of Amorphous High-k  $\text{LaGdO}_3$  Films, S. P. Pavunny, R. Thomas, and R. S. Katiyar, *ECS Transactions*, 45, 219 (2012).
97. Ferroelectric-Carbon Nanotube Memory Devices, Ashok Kumar, Sai G. ShivaReddy, Margarita Correa, Oscar Resto, Youngjin Choi, Ram. S. Katiyar, James. F. Scott, Gehan A. J. Amarantunga, Haidong Lu, Alexe. Gruverman, *Nanotechnology*, 23, 165702 (2012).
98. Microstructure-relaxor property relationship of  $\text{PbSc}_{0.5}\text{Nb}_{(1-x)/2}\text{Ta}_{x/2}\text{O}_3$  thin films, Margarita Correa, Ashok Kumar, and R. S. Katiyar, *Ferroelectrics*, 426, 112 (2012).
99. Local vibrational modes and Fano interaction in p-type  $\text{ZnO}$ : Sb system. K Samanta, A K Arora and R S Katiyar. *J. Phys. D: Appl. Phys.* 45 (2012) 185304 (5pp).
100. Impedance spectroscopy analysis of  $\text{Ba}_{0.7}\text{Sr}_{0.3}\text{TiO}_3/\text{La}_{0.7}\text{Sr}_{0.3}\text{MnO}_3$  heterostructure, R. Martínez, Ashok Kumar, R. Palai, J. F. Scott, and R. S. Katiyar, *J. App. Phys.D*, 44,105302 (2011).
101. Effect of the periodicity and the composition in artificially  $\text{BaTiO}_3/(\text{Ba},\text{Sr})\text{TiO}_3$  superlattices, N. Ortega, Ashok Kumar, O. A. Maslova, Yu. I. Yuzyuk, J. F. Scott, and R. S. Katiyar, *Phys. Rev. B*, 83 144108 (2011)
102. Phonon anomalies near the magnetic phase transitions in  $\text{BiFeO}_3$  thin films with rhombohedral R3c symmetry, Manoj K. Singh and R. S. Katiyar, *J. App. Phys.*, 109, 07D916 (2011).
103. Magnetic control of ferroelectric interfaces, S. Dussan, Ashok Kumar, R. S. Katiyar, Shashank Priya, and J. F. Scott, *J. Phys.: Condens. Matter*, 23 202203 (2011)
104. Fabrication and electrical characterization of high-k  $\text{LaGdO}_3$  thin fields and field effect transistors, S.P.Pavunny, R. Thomas, T.S. Kalkur, J. Schubert, E. Fachini, and R.S. Katiyar, *Proceedings of ECS Transactions, Silicon Compatible Materials, Processes, and Technologies for Advances Integrated Circuits and Emerging Applications*, 35 [2], 297, (2011)
105. Magneto-electric coupling in  $\text{PbZr}_{0.53}\text{Ti}_{0.47}\text{O}_3/\text{CoFe}_2\text{O}_4$  layered thin films, N. Ortega, Ashok Kumar, C. Rinaldi, and R. S. Katiyar, *Integrated Ferroelectric* 124, 33 (2011)
106. Optical properties of  $\text{In}_2\text{O}_3$  octahedra nano-beads grown on  $\text{ZnO}$  nanowires, Satyaprakash Sahoo, A.P.S. Gaur, A.K. Arora, and R.S. Katiyar, *Chemical Physics Letter*, 510, 242 (2011)
107. Transition metal modified bulk  $\text{BiFeO}_3$  with improved magnetization and linear magneto-electric coupling, Venkata Sreenivas Puli, Ashok Kumar, Neeraj Panwar, I. C. Panwar, and R. S. Katiyar, *Journal of Alloys and Compounds*, 509, 8223 (2011)

108. Synthesis, structural, and magnetic properties of Ni-doped  $\text{In}_2\text{O}_3$  nanoparticles, Sandra Dussan, M. K. Singh, Ashok Kumar, and R. S. Katiyar Integrated Ferroelectrics 125, 155 (2011)
109. Investigation of multiferroic properties of  $(\text{PbZr}_{0.53}\text{Ti}_{0.47}\text{O}_3)(1-x)-(\text{PbFe}_{0.5}\text{Ta}_{0.5}\text{O}_3)x$  ceramics, Dilsom A. Sánchez, Ashok Kumar, Nora Ortega, Ricardo Martínez, and R. S. Katiyar, Integrated Ferroelectrics 124, 61 (2011)
110. Anomalous enhancement in magnetization of  $\text{BiFeO}_3 - \text{CoFe}_2\text{O}_4$  heterostructure multilayer thin films deposited on  $\text{SrTiO}_3$  with different orientation, Sandra Dussan, Manoj K. Singh, R. S. Katiyar, Integrated Ferroelectrics 124, 73 (2011)
111. Self-assembled highly uniform  $\text{ZnO}$  sub-micron rods on metal grid growth by vapor-liquid-solid method, Satyaprakash Sahoo, J. F. Scott, Akhilesh Arora, and R. S. Katiyar, Crystal Growth & Design, 11 (8); 3642 (2011)
112. Polarized Raman scattering in monolayer, bilayer, and suspended bilayer graphene, Satyaprakash Sahoo, R. Palai, and R.S. Katiyar, J. App. Phys., 110, 044320 (2011)
113. Photovoltaic effect in a wide-area semiconductor-ferroelectric device, R.K. Katiyar, Ashok Kumar, G. Morell, J.F. Scott, and R.S. Katiyar, App. Phys. Lett., 99, 092906 (2011)
114. Electric control of magnon, phonon and magnetic moment in  $\text{BiFeO}_3$ : direct evidence of magneto-electric coupling, Ashok Kumar, J.F. Scott, and R.S. Katiyar, App. Phys. Lett., 99, 062504 (2011)
115. Biferroic relaxors, Ashok Kumar, J.F. Scott, and R.S. Katiyar, App. Phys. Lett., 99, 042907 (2011)
116. Symmetries and multiferroic properties of new room-temperature magnetoelectrics: lead iron tantalate-lead zirconate titanate (PFT/PZT), Dilsom A. Sánchez, N. Ortega, Ashok Kumar, R. Roque-Malherbe, R. Polanco, J. F. Scott, and R. S. Katiyar, AIP Advances, 1, 042169 (2011).
117. Direct observation of fatigue in epitaxially grown  $\text{Pb}(\text{Zr},\text{Ti})\text{O}_3$  thin films using second harmonic piezoresponse force microscopy, Nishit M. Murari, Seungbum Hong, Ho Nyung Lee, and R.S. Katiyar, Applied Physics Letter, 99, 052904 (2011)
118. Studies of photovoltaic properties of nanocrystalline thin films of  $\text{CdS}-\text{CdTe}$ , Rajesh K. Katiyar, Satyaprakash Sahoo, A.P.S. Gaur, Arun Kumar Singh, G. Morell and R.S. Katiyar, J. of Alloys and Compounds, 509 [41], 10003 (2011)
119. Absence of magnetism in Cr-doped  $\text{In}_2\text{O}_3$ : A case study of phase separation versus phase formation, Anand P.S. Gaur, Satyaprakash Sahoo, R.K. Katiyar, Carlos Rinaldi, J.F. Scott, and R.S. Katiyar, Journal of Applied Physics D, 44, 495002 (2011)
120. Investigation on Room Temperature Multiferroic Bi-Relaxor, Ashok Kumar, J.F. Scott, and, Ram S.Katiyar, Integrated Ferroelectrics, 131, 110, (2011).
121. Optical properties of amorphous high-k  $\text{LaGdO}_3$  films and its band alignment with Si, S. P. Pavunny, R. Thomas, A. Kumar, E. Fachini, and R. S. Katiyar, Journal of Applied Physics 111, 044106 (2012).
122. Ferroelectric and Dielectric properties of  $\text{BaTiO}_3/\text{Ba}_{0.30}\text{Sr}_{0.70}\text{TiO}_3$  Superlattices. N. Ortega, Ashok Kumar, Yu. I. Yuzyuk, J. F. Scott and Ram S. Katiyar. Integrated Ferroelectrics 134, 1-7 (2012).
123. Effect of Vanadium Ions on the Functional Properties of Nanocrystalline Zinc Oxide. Marco A. Gálvez Saldaña, Oscar Perales Perez and Maxime J-F Guinel. Material Research Society Proceedings, 1368, mrss11-1368-ww11-12 doi:10.1557/ opl.2011.1038 (2011)
124. Tuning of Magnetic Properties in Cobalt-Doped Nanocrystalline Bismuth Ferrite. Gina Montes Albino, Oscar Perales-Pérez, Boris Renteria, Marco Galvez and Maxime J-F Guinel (2011). Material Research Society Proceedings, 1368 , mrss11-1368-ww11-35 doi:10.1557/ opl.2011.1023
125. Palladium Nanoshell Catalysts Synthesis on Highly Ordered Pyrolytic Graphite for Oxygen Reduction Reaction, Lisandra Arroyo-Ramírez, Diego Rodríguez, Wilfredo Otaño, and Carlos R. Cabrera, ACS Appl. Mater. Interfaces, 4 (4), 2018 (2012).

126. Synthesis and electrocatalytic oxygen reduction activity of graphene-supported Pt<sub>3</sub>Co and Pt<sub>3</sub>Cr alloy nanoparticles, Chitturi Venkateswara Rao, Arava Leela Mohana Reddy, Yasuyuki Ishikawa and Pulickel M. Ajayan, *Carbon* 49 (2011) 931.

127. Free standing graphene-diamond hybrid films and their electron emmision properties, Deepak Varshney, Chitturi Venkateswara Rao, Maxime J-F Guinel, Yasuyuki Ishikawa, Brad R. Weiner, Gerardo Morell, *J. Appl. Phys.*, 11 (2011) 044324.

128. Structural and Optical Propertiesof Zn<sub>1-x</sub>Cu<sub>x</sub>O Thin Films. Ram S. Katiyar and Kousik Samanta. *Handbook of Zinc Oxide and Related Materials: Volume One, Materials / Chapter 12* (2012). (Review Article).

129. Low temperature synthesis and Raman scattering of Mn-doped ZnO nanopowders Boqian Yang, Ashok Kumar, Noel Upia, Peter Feng, and R. S. Katiyar, *Journal of Raman Spectroscopy*, 41, 88, (2010)

130. Raman Spectroscopy and Field Emission characterization of Delafossite CuFeO<sub>2</sub>, S. P. Pavunny, Ashok Kumar, and R.S. Katiyar, *J. App. Phys.*, 107, 013522 (2010)

131. Investigation on (Sr,Co)Bi2Nb2O9 thin films: A lead free room temperature multiferroics, Ashok Kumar, Bryan Collazo, D. Sánchez, and R. S. Katiyar, *Physica Status Solidi B:Rapid Research Letters*, 4, 25 (2010)

132. Phonon spectroscopy near phase transition temperatures in multiferroic BiFeO<sub>3</sub> epitaxial thin films, R. Palai, J. F. Scott, and R. S. Katiyar, *Phy. Rev. B*, 81, 024115 (2010)

133. Raman spectroscopy of single-domain multiferroic BiFeO<sub>3</sub>, R. Palai, H. Schmid, J. F. Scott, and R. S. Katiyar, *Phy. Rev. B*, 81, 064110 (2010)

134. Magnetic effects on dielectric and polarization behavior of multiferroic heterostructures, S. Dussan, Ashok Kumar, J. F. Scott, and R. S. Katiyar, *App. Phys. Lett.*, 96, 072904 (2010)

135. Study of physical properties of integrated ferroelectric/ferromagnetic heterostructures, R. Martínez V. Ashok Kumar, R. Palai, R. S. Katiyar, and J. F. Scott, *J. Appl. Phys.* 107, 114107, (2010)

136. Fabrication and characterization of artificially designed PZT/LSMO heterostructure, S. Dussan, Ashok Kumar, and R. S. Katiyar, *Mater. Res. Soc. Symp. Proc.*, 1199, 1199-F03-05 (2010)

137. Structural and magnetoelectric properties of pulsed laser deposited ferroelectric/ferromagnetic heterostructures, R. Martínez V. Ashok Kumar, R. Palai, and R. S. Katiyar, *Mater. Res. Soc. Symp.Proc.*, 1199, 1199-F03-04 (2010).

138. Liquid Injection MOCVD Grown Binary Oxides and Ternary Rare-Earth Oxide as Alternate Gate-Oxides for Logic Devices, R. Thomas, P. Ehrhart, R. Waser, J. Schubert, A. Devi, and R. S. Katiyar, *ECS Transactions*, 33 (3) 211 (2010)

139. Nanoscale ordering and multiferroic behavior in Pb(Fe<sub>1/2</sub>Ta<sub>1/2</sub>)O<sub>3</sub>, R. Martínez, R. Palai, H. Huhtinen, J. Liu, J. F. Scott, and R. S. Katiyar, *Phys. Rev. B*, 82, 134104 (2010)

140. Fabrication and characterization of relaxor ferroelectric PbFe1/2Ta1/2O3 thin film: A comparison with ceramics, R. Martínez V., Ashok Kumar, Dilsom A. Sanchez, R. Palai, and R. S. Katiyar, *J. Appl. Phys.* 108, 084105 (2010)

141. Fabrication and characterization of the multiferroic bi-relaxor lead-iron-tungstate/lead-zirconate-titanate, Ashok Kumar, j. F. Scott, and R. S. Katiyar, *J. Appl. Phys.* 108, 064105 (2010)

142. Raman scattering studies of p-type Sb-doped ZnO thin films, K. Samanta, P. Bhattacharya, and R. S. Katiyar, *J. App. Phys.*, 108, 113501 (2010)

143. Near room temperature relaxor multiferroic, Dilsom A. Sánchez, Ashok Kumar, Nora Ortega, R. S. Katiyar, and J. F. Scott, *App. Phys. Lett.*, 97, 202910 (2010).

144. Room-temperature multiferroic effects in superlattice nano-capacitors, S. Dussan, Ashok Kumar, S.Priya, J. F. Scott and R. S. Katiyar, *Applied Physics Letters*, 97, 252902 (2010).

145. Novel room temperature magnetoelectric Multiferroics for Random Access Memory Elements, Ashok Kumar, J. F. Scott and R. S. Katiyar, *IEEE Transactions Ultrasonics, Ferroelectrics, and Frequency Control*, 57, 2237, (2010).

146. Investigation of temperature dependent polarization, dielectric, and magnetization behavior of multiferroic layered nanostructure, N. Ortega, Ashok Kumar, C. Rinaldi, and R. S. Katiyar, *Thin Solid Films*, 519, 641, (2010).

147. Palladium Nanostructures Synthesis by Sputtering Deposition on HOPG Surfaces, L. Arroyo-Ramírez, Y. Figueroa, D. Rodríguez, W. Otaño, and C. R. Cabrera, *ECS Transactions* - 217th ECS Meeting, Vancouver, Canada, Volume 28, August, 2010.

148. Structural and Magnetic Properties of  $Zn_{1-x}Co_xO$  Nanoparticles Prepared by a Simple Sol-Gel Method at Low Temperature, S.R. Jáuregui-Rosas, O. Perales-Perez, S. Urcia-Romero, M. Asmat-Uceda, and E. Quezada-Castillo, *Mater. Res. Soc. Symp. Proc.* Vol. 1201, 1201-H10-34, (2010).

149. Effect of Co- and Sc-doping on the functional properties of nanocrystalline powders and thin films of  $ZnO$ , M. Galvez, O. Perales-Perez and S. P. Singh, *Materials Research Society Proceedings*, Vol. 1256- N11- 23 (2010).

150. Synthesis and magnetic properties of pure and Co-doped nanocrystalline bismuth ferrite, G. Montes, O. Perales-Pérez, B. Renteria, and M. Galvez, *Materials Research Society Proceedings*, Vol. 1256- N06- 14 (2010).

151. Growth and field emission study of monolithic carbon nanotube/ diamond composite, Deepak Varshney, Brad R. Weiner, and Gerardo Morell, *Carbon*, 48, 3353, (2010).

152. Room temperature ferromagnetism in spin-coated Anatase and Rutile  $Ti_{1-x}M_xO_2$  ( $M= Fe, Mn, Co$ ) films, D. Barrionueva, S.P. Singh, and M.S. Tomar, *Mater. Res. Symp. Proc.* Vol. 1201, 1201-H10-07 (2010).

153. Silicon Encapsulated Carbon Nanotubes, Sri Lakshmi Katar, Azlin Biaggi-Labiosa, Amairy E. Plaud, Edgar Mosquera-Vargas, Luis F Fonseca, Brad R. Weiner, Gerardo Morell, *Nanoscale Research Letters* 5, 74 (2010).

154. SiN/Bamboo like Carbon Nanotube Composite Electrodes for Lithium Ion Rechargeable Batteries, Sri Lakshmi Katar, Dione Hernandez, Azlin Biaggi-Labiosa, Edgar Mosquera-Vargas, Luis Fonseca, Brad R. Weiner, Gerardo Morell, *Electrochimica Acta* 55, 2269 (2010).

155. Sputtering configurations and the luminescence of rare earths-doped silicon rich oxide thin films. C Rozo, L F Fonseca, *Optical Materials* 32, 576 (2010).

156. In-situ TEM-STM Observations of SWCNT Ropes-tubular Transformations, F Sola, M Lebron-Colon, P J Ferreira, L F Fonseca, M A Meador, and C Marin, *Mat. Res. Soc. Symp. Proc.* 1204, K10.26 (2010).

157. Structural, optical and magnetic properties of Co-doped  $ZnO$  nanopowders, Segundo R. Jáuregui-Rosas, Oscar J. Perales-Perez, Lourdes A. Noriega and Luis A. Castillo, *Materials Research Society Proc.*, Vol. 1292, DOI: 10.1557/ opl2011.9, (2011).

158. Electron emission from diamond films seeded using kitchen-wrap polyethylene, Deepak Varshney, Vladimir I. Makarov, Puja Saxena, Maxime J-F Guinel, Ashok Kumar, James F. Scott, Brad R. Weiner, and Gerardo Morell, *J. Phys. D: Appl. Phys.*, 44, 085502, (2011).

159. Structural, Magnetic, and Electrical properties of  $BiFe_{1-x}Mn_xO_3$  thin films, D. Barrionueva, S.P. Singh, and M.S. Tomar, *Mater. Res. Symp. Proc.* (2011)

160. Fabrication and field emission study of novel rod-shaped diamond-like carbon nanostructures, Deepak Varshney, Vladimir I. Makarov, Puja Saxena, James F. Scott, Brad R. Weiner, and Gerardo Morell, A. Gonzalez-Berrios, *Nanotechnology*, 21, 285301, (2011).

161. Phonon anomalies and phonon-spin coupling in multiferroic  $PbFe_{0.5}Nb_{0.5}O_3$  thin film, M. Correa, Ashok Kumar, S. Priya, J. F. Scott and R. S. Katiyar, *Physical Review B*, 83, 014302 (2011).

163. Structural and Luminescence Properties of Nanocrystalline Eu<sup>3+</sup>-doped Gd<sub>2</sub>O<sub>3</sub>, S. Jauregui, O. Perales-Perez, E. Fachini, W. Jia, Mater. Res. Soc. Symp. Proc. Vol. 1074, 1074-I10-41, (2009).
164. Optical and luminescent properties of highly oriented nanocrystalline Gd<sub>2-x</sub>Eu<sub>x</sub>O<sub>3</sub> thin films, S. Jáuregui-Rosas, O. Perales Pérez, S. P. Singh, M.S. Tomar, W. Jia, and O. Vásquez, Mater. Res. Soc. Symp. Proc. Vol. 1111, D04-11, (2009)
165. Structural, Optical and Luminescent properties of ZnO:Eu nanocrystals prepared by sol-gel method, S. Jáuregui-Rosas, O. Perales Pérez, W. Jia, O. Vasquez and L. Angelats, Mater. Res. Soc. Symp. Proc., Vol 1174, 1174-V09-07, (2009).
166. Positive temperature coefficient of resistivity and negative differential resistivity in lead iron tunstate-lead zirconate titanate Ashok Kumar, R.S. Katiyar, and J. F. Scott, Applied Physics Letters 94, 212903 (2009)
167. Structural, electrical and magnetic properties of chemical solution deposited BiFe<sub>1-x</sub>Ti<sub>x</sub>O<sub>3</sub> and BiFe<sub>0.9</sub>Ti<sub>0.05</sub>Co<sub>0.05</sub>O<sub>3</sub> thin films, N. M. Murari, R. Thomas, R. E. Melgarejo, S. P. Pavunny, and R. S. Katiyar, J. Appl. Phys. 106, 014103, (2009)
168. Microstructural and ferromagnetic properties of Zn<sub>1-x</sub>Cu<sub>x</sub>O thin films, K. Samanta, P. Bhattacharya, and R. S. Katiyar, J. Appl. Phys. 105, 113929, (2009)
169. Magnetic control of large room-temperature polarization, Ashok Kumar, G. L. Sharma, R.S. Katiyar, R. Pirc, R. Blinc, and J. F. Scott, Journal of Physics: Condensed Matter, 21, 382204, (2009)
170. Metalorganic chemical vapor deposited DyScO<sub>3</sub> buffer layer in Pt/Bi<sub>3.25</sub>Nd<sub>0.75</sub>Ti<sub>3</sub>O<sub>12</sub>/DyScO<sub>3</sub>/Si metal-ferroelectric-insulator-semiconductor diodes, R. Thomas, R. E. Melgarejo, N. M. Murari, S. P. Pavunny, and R. S. Katiyar, Solid State Communications, 149, 2013, (2009)
171. Temperature-Dependent Structural Disintegration of Delafossite CuFeO<sub>2</sub>, Shojan P. Pavunny, Ashok Kumar, N.M. Murari, R. Thomas, and R.S. Katiyar, Mater. Res. Soc. Symp. Proc., 1183, 1183-FF06-14 (2009)
172. Dynamic magneto-electric multiferroics PZT/CFO multilayered nanostructure, Ashok Kumar, N. Ortega, and R. S. Katiyar, J. Mater. Sci., 44, 5127 (2009)
173. Effect of Mn substitution on electrical and magnetic properties of Bi<sub>0.9</sub>La<sub>0.1</sub>FeO<sub>3</sub>, Dillip K. Pradhan, R. N. P. Choudhary, C. Rinaldi, and R. S. Katiyar, J. App. Phys., 106, 024102, (2009)
174. Anomalous magnetic ordering induced spin-phonon coupling in BiFeO<sub>3</sub> thin films, Manoj J. Singh, W. Prellier, Hyun M. Jang, and R.S. Katiyar, Solid State Communication, 149, 1971, (2009)
175. Desing and Development of Multiferroic Relaxors and Layered Nanostructured Thin Films, Ashok Kumar, Margarita Correa, N. Ortega, and R. S. Katiyar, Recent Advances in Dielectric Materials, Edited by Ai Huang ISBN 978-1-60692-266-8, 2009 Nova Publishers Inc, Book Chapter (2009)
176. First-principles computational study on transition metal oxide substitution at ZnO/MgO interface, J. J. Saavedra-Arias, J. Velez, Y. Ishikawa, and R. S. Katiyar, American Chemical Society (ACS) Southeastern Regional Meeting Proceedings, San Juan, Puerto Rico, (October 21-24, 2009)
177. Relaxed Coupling J. Phys. Condens. Ashok Kumar, R. S. Katiyar, and J. F. Scott, Nature Materials:Research highlights 8, 772 (2009), DOI: 10.1038/nmat2536
178. Multiferroics phenomenon in Pb(B'B'')O<sub>3</sub> relaxor thin films and ceramics, R.S. Katiyar, Ashok Kumar, Margarita Correa, and I. Rivera, MS&T08 (Material Science and Technology 2008 Conference and Exhibition Proceedings, Perovskite Oxides: Films, Nanostructure, Properties, and Applications) 293-300, (2008)
179. Multiferroics Relaxor Pb(Fe<sub>0.66</sub>W<sub>0.33</sub>)<sub>0.80</sub>Ti<sub>0.20</sub>O<sub>3</sub> thin films, Ashok Kumar, and R.S. Katiyar, MS&T08 (Material Science and Technology 2008 Conference and Exhibition Proceedings, Fabrication, Microstructure and Interfacial Properties of Multifunctional Oxides Thin Films) 144-151, (2008)
180. Polarized Raman scattering of multiferroic BiFeO<sub>3</sub> single domain crystal and thin films, R. Palai, H. S. Schmid, and R. S. Katiyar, 17th IEEE International Symposium on the Applications of Ferroelectrics (ISAF), 2, 10.1109/ISAF.2008.4693780 (2008)
181. Synthesis and Characterization of Nanocrystalline Eu<sup>3+</sup>-doped Gd<sub>2</sub>O<sub>3</sub>, S. Jauregui, O. Perales-Perez, E. Fachini, W. Jia, NANOTECH Technical Proceedings, 1, 990, 2008

**US Patent**

1. Micro and nanoscale magnetoelectric multiferroic lead iron tantalate-lead zirconate titanate, R. S. Katiyar, A. Kumar, N. P. Ortega, D. A. Sanchez, J. F. Scott, D. M. Evans, and J. M. Gregg, US Patent# US9299485 B1, Mar 29, 2016.